Structure and shearing conditions in the Day Nui Con Voi massif: Implications for the evolution of the Red River shear zone in northern Vietnam

R. Anczkiewicz,[1] G. Viola,[2] O. Müntener,[3] M. F. Thirlwall,[4] Igor M. Villa,[5,6] and Nguyen Quoc Quong[1]

Received 24 March 2006; revised 21 August 2006; accepted 14 November 2006; published 1 March 2007.

[1] The Day Nui Con Voi massif bears a record of the Red River shear zone (RRSZ) activity in North Vietnam. It forms a large-scale antiformal ''core complex''-type structure, bounded by the Song Hong and Song Chay faults. The kinematics of both faults are identical and reflect transtensional shear initiated under upper amphibolite facies conditions and propagated into greenschist facies. Microfabric analysis establishes that both extensional and strike-slip shearing initiated between 700 and 500°C. The RRSZ evolved from a single, subvertical fault, which, due to strike-perpendicular extension, underwent progressive dilation. The created space was ''intruded'' by already metamorphosed and deformed ductile middle crust in the form of a gneissic ''dome.'' Both strike-slip and extensional shearing were accommodated in the limbs of the antiform, while its core was uplifted from midcrustal level bearing only a minor record of sinistral shear.
Citation: Anczkiewicz, R., G. Viola, O. Müntener, M. F. Thirlwall, I. M. Villa, and N. Q. Quong (2007), Structure and shearing conditions in the Day Nui Con Voi massif: Implications for the evolution of the Red River shear zone in northern Vietnam, *Tectonics*, *26*, TC2002, doi:10.1029/2006TC001972.

1. Introduction

[2] It has long been proposed that a significant amount of India-Asia postcollisional convergence was accommodated by lateral extrusion of lithospheric blocks along deeply rooted, large-scale strike-slip shear zones, among which the Red River shear zone (RRSZ) serves as a model example [e.g., *Tapponnier et al.*, 1982, 1990]. This model has been widely accepted and Tertiary geology of SE Asia has been predominantly interpreted in the context of ''escape tectonics'' and of the Red River shear zone evolution in particular. The lithospheric extrusion model was challenged by *Burchfiel et al.* [1989], *Wang and Burchfiel* [1997] and by *Jolivet et al.* [2001], who interpreted the RRSZ as a fault acting mainly in the upper crust while being detached at midcrustal depth. Their models thus partially diminish the crustal-scale relevance of the escaping blocks' bounding faults and of the RRSZ in particular. Moreover, studies by *Jolivet et al.* [1999] and *Jolivet et al.* [2001] demonstrated a greater significance of extensional structures in the Tertiary evolution of the Indochina block than previously thought, indicating that it did not behave as a rigid body during the extrusion process but also underwent significant internal deformation.

[3] The metamorphic conditions of shearing are also contentious. *Leloup et al.* [2001] estimated that RRSZ strike-slip shearing occurred at temperatures exceeding 700°C, while *Jolivet et al.* [2001] argued that RRSZ-related metamorphism was restricted to greenschist facies conditions. Thus both the role of the RRSZ in the collisional process and the associated conditions of shearing remain highly controversial.

[4] In this study we focus on the structure, kinematics and shearing conditions of the Day Nui Con Voi massif (DNCV), which delineates the RRSZ in North Vietnam and southern Yunnan (China). We document that it was emplaced in an overall transtensional regime, which led to the vertical extrusion of the ductile middle crust as an antiformal dome.

2. Overview of the Red River Shear Zone Geology

[5] The RRSZ strikes for about 1000 km from SE Tibet to the South China Sea (Figure 1). It is one of the major continental discontinuities in SE Asia, which separates the south China block from the Indochina block and is believed to have had a major impact on the Tertiary tectonic evolution of SE Asia. The trend of the RRSZ is defined by four narrow, elongated metamorphic belts: the Xuelong Shan, Diancang Shan, Ailao Shan and the Day Nui Con Voi (Figure 1). They are characterized by a generally steeply dipping foliation (except for the DNCV, see below) and subhorizontal stretching lineation. Evidence for left-lateral shear was presented extensively by *Tapponnier et al.* [1986]

[1]Institute of Geological Sciences, Polish Academy of Sciences, Kraków Research Centre, Kraków, Poland.
[2]Geological Survey of Norway, Trondheim, Norway.
[3]Institute of Mineralogy and Geochemistry, University of Lausanne, Lausanne, Switzerland.
[4]Department of Geology, Royal Holloway, University of London, Egham, UK.
[5]Institut für Geologie, Universität Bern, Bern, Switzerland.
[6]Also at Dipartimento di Scienze Geologiche, Università di Milano Bicocca, Milan, Italy.

0278-7407/07/2006TC001972

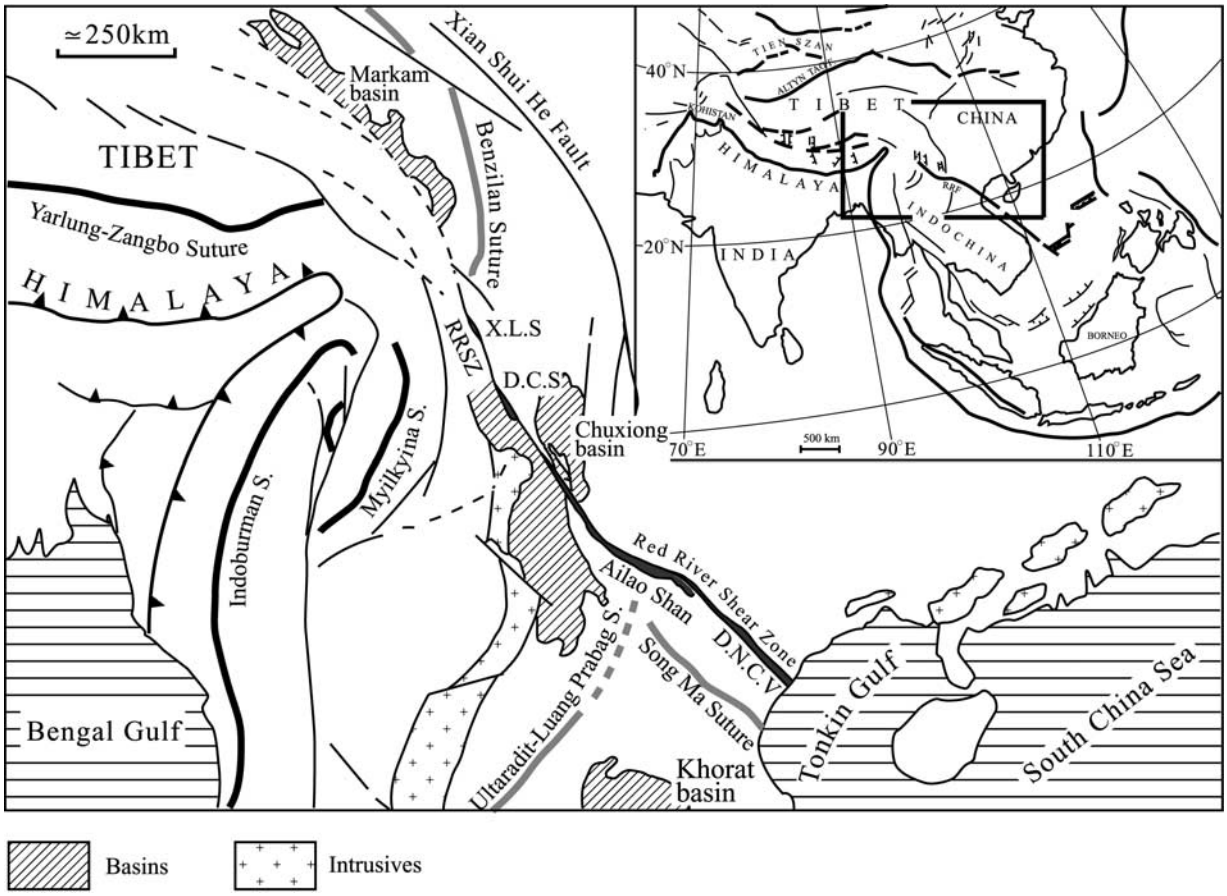

Figure 1. Tectonic sketch of SE Asia (based on the work by *Leloup et al.* [1995]). The Red River shear zone is defined by four elongated metamorphic massifs: XLS, Xuelong Shan; DCS, Diancang Shan; DNCV, Day Nui Con Voi.

and *Leloup et al.* [1995, 2001], who reported remarkably consistent kinematics along the entire fault length. The amount of sinistral displacement was estimated at about 700 ± 200 km, with 3 to 5 cm/yr slip rates [*Leloup et al.*, 1995]. Peak metamorphic conditions were established as ~700°C and 0.70 ± 0.15 GPa, whereas retrograde parageneses developed at temperature of ~480°C and pressure of 0.3 GPa [*Nam et al.*, 1998; *Leloup and Kienast*, 1993; *Leloup et al.*, 2001]. On the basis of analogue modeling results, *Tapponnier et al.* [1982] proposed that the South China Sea had formed as a pull-apart basin kinematically linked with the RRSZ. This model found support in the geochronological data, which indicate that the formation of the South China Sea basin and the left-lateral motion along the RRSZ took place during the Oligo-Miocene [e.g., *Briais et al.*, 1993; *Schärer et al.*, 1994; *Gilley et al.*, 2003; *Leloup et al.*, 2001].

[6] Since circa 5 Ma the sense of movement along the Red River fault has been oblique right-lateral with a dip-slip component [e.g., *Leloup et al.*, 1995; *Replumaz et al.*, 2001; *Schoenbohm et al.*, 2004].

[7] The timing of the RRSZ activity is constrained by geochronological data obtained predominantly from the Chinese part of the shear zone. Geochronometers with high closure temperature point to the Oligo-Miocene as a major period of RRSZ activity. U-Pb dating of zircon, monazite and titanite from deformed granitoids within the southern Ailao Shan massif yielded ages between 33 and 22 Ma, which were interpreted as related to the sinistral strike-slip motion [*Zhang and Schärer*, 1999]. This time interval of the RRSZ activity was confirmed by in situ Th-Pb monazite dating by *Gilley et al.* [2003], who reported monazite ages between 34 and 21 Ma. On the basis of textural evidence the latter authors interpreted the obtained ages as representing synkinematic (relatively to the sinistral shear phase) monazite and garnet growth in the Ailao Shan massif. The same study also revealed a rather complex thermal history of the DNCV massif, with monazites demonstrating strong inheritance problems with age components from 210 to 21 Ma [*Gilley et al.*, 2003].

[8] Because of the high-temperature conditions within the metamorphic massifs delineating the RRSZ, the vast majority of available isotopic ages reflect postmetamorphic cooling. Numerous Ar-Ar and K-Ar dating results obtained for the DNCV show a wide range of ages. Hornblende dates span between 34 and 27 Ma, while feldspars display rather

complex age spectra defining ages clustering around 30 and 23 Ma [*Nam et al.*, 1998; *Wang et al.*, 1998, 2000; *Leloup et al.*, 2001]. Relatively few muscovite Ar-Ar dates vary from 33 to 24 Ma [*Wang et al.*, 1998, 2000; *Maluski et al.*, 2001]. Biotite ages tend to cluster around 23–26 Ma [e.g., *Nam et al.*, 1998; *Harrison et al.*, 1996; *Leloup et al.*, 2001; *Wang et al.*, 2000; *Garnier et al.*, 2002], which probably is the best estimate of the time when DNCV rocks cooled below the closure temperature for the Ar-Ar system in biotite. The final cooling phase, which is commonly accepted as coinciding with the termination of significant sinistral movement along the RRSZ, is constrained by apatite fission track ages between 30 and 25 Ma [*Viola and Anczkiewicz*, 2007].

3. Structure and Metamorphism of the Red River Shear Zone in North Vietnam

[9] The RRSZ in North Vietnam is defined by the Day Nui Con Voi massif and by the southernmost part of the Ailao Shan massif (Figure 2a). The Vietnamese part of the Ailao Shan massif is composed mainly of granite gneisses and granites with minor slivers of metasediments. The DNCV is a NW–SE trending narrow belt up to about 20 km wide and 270 km long (Figure 1). It is bounded to the SW by the SW dipping Song Hong fault and to the NE by the NE dipping Song Chay fault (Figure 2a). The massif is composed of garnet sillimanite gneisses (locally migmatitic), amphibolites, leucogranites, smaller amounts of garnet mica schists and marbles. They commonly display mylonitic, rarely ultramylonitic textures. Along the Song Hong (SH) and the Song Chay faults (SC) sedimentary basins developed, which are filled with detrital material of Neogene age [*General Geological Department of the Democratic Republic of Vietnam*, 1973]. The basins are bounded by the DNCV gneisses on one side and by Paleozoic low-grade metamorphic rocks on the other (Figure 2a).

[10] Our studies were carried out virtually along the whole Vietnamese part of the DNCV massif and its vicinity. Below we present our structural interpretation of the DNCV massif and document its metamorphic conditions in relation to the dominant structural features.

3.1. Day Nui Con Voi Massif

[11] The investigated area spreads between Viet Tri in the south and Laocai in the north (Figure 2a). The northern part of the DNCV massif is usually much better exposed and most of the observations presented here come from the region between Yen Bai and Ba Xat (Figure 2a). Because of difficult access and lack of outcrops, the inner part of the DNCV was particularly difficult to investigate. However, two recent road cuts (see auxiliary material[1] Table S1 for GPS coordinates) provided nearly continuous exposures, which enabled us to obtain detailed structural information across the entire massif.

[12] To a first order, the DNCV massif is a large-scale antiform bounded by the steeply dipping SH and SC faults (Figures 3a and 3b). Although the metamorphic conditions recorded across the entire antiform are similar (see below), deformation is strongly partitioned between its core and margins. In sections 3.1.1 and 3.1.2 we discuss these two structural domains separately and then present their integrated kinematic interpretation.

3.1.1. Deformation Along the Margins of the DNCV: Song Hong and Song Chay Fault Zones

[13] Deformation along the boundaries of the DNCV massif is strongly partitioned within the SH and SC faults. The earliest observed deformation phase is defined by a pervasive gneissic foliation and compositional banding within amphibolites underlined by quartzofeldspathic and amphibole rich layers (Figures 4a and 4b). Foliation planes in the gneisses are defined by biotite, sillimanite and muscovite as well as flattened quartzofeldspathic minerals, which flow around usually strongly flattened garnet porphyroclasts. Rocks often display mylonitic, rarely ultramylonitic textures (Figures 4a–4e), which is a general feature observed along the entire length of the fault [e.g., *Leloup et al.*, 1995]. The metamorphic foliation generally dips steeply and bears stretching lineations that parallel the strike of the belt. The lineation is commonly subhorizontal, although it can locally plunge up to 30° toward the northwest or southeast (Figure 2c). Kinematic indicators on all scales consistently point to left-lateral shear (Figures 4a–4f). Locally, symmetric upright folds (on the centimeter to tens of meters scale), with axes parallel to the stretching lineation, are present (Figures 2d, 3c, and 5a). Although these folds deform the regional gneissic foliation, kinematic indicators are consistently left lateral in both limbs. The same observation applies to the SH and SC faults, which bound the large-scale antiform. Kinematic indicators associated with these faults show very clear and consistent sinistral shear (Figures 4a–4f). In the gneisses, penetrative on outcrop scale, axial-planar cleavage associated with these folds is often injected by thin intrusions of leucogranites (up to 20 cm, usually a few centimeters), indicating high-temperature and large melt production during this deformation phase. In the garnet micaschists mapped in the Thai Nien area, this axial planar cleavage becomes the dominant foliation (Figure 3c).

[14] An important structural feature confined only to the vicinity of the SH and SC faults are NW–SE trending asymmetric folds (parallel to the main stretching lineation) characterized by subhorizontal to gently dipping axial planes (Figures 2e, 5b, and 5d–5g). They occur on up to several meters scale and show NE vergence in the vicinity of the SC fault and SW vergence in the vicinity of SH fault (Figure 3a). They deform the DNCV mylonitic foliation. A distinct second generation of stretching lineations is locally found oriented at high angle to the axes of these folds. Associated kinematic indicators, such as feldspar sigma clasts (Figure 5c) or shear bands, confirm shearing along the limbs of the folds in a direction perpendicular to their axes. This is in turn consistent with the observed fold vergence, i.e., top-to-the-NE and SW for the SC and SH faults, respectively. Examples of these folds can be observed along the limbs of the large-scale DNCV antiform

[1] Auxiliary materials are available at ftp://ftp.agu.org/apend/tc/2006tc001972.

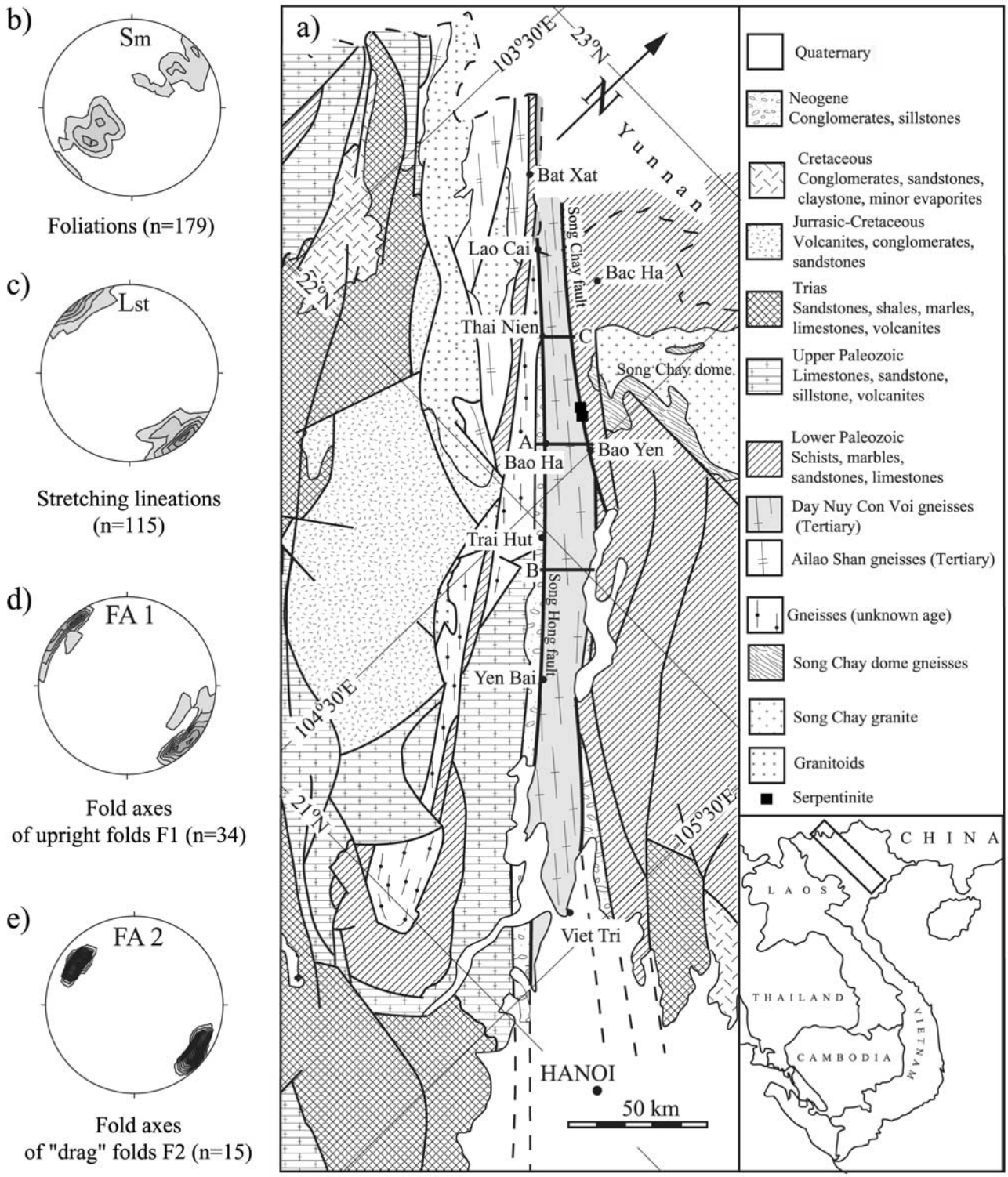

Figure 2. Simplified geological map of northern Vietnam (based on map by *General Geological Directorate* [1978]). Lines A-C mark the position of the cross sections presented in Figure 3. Stereonets are equal-area, lower hemisphere projections of the Day Nui Con Voi massif (a) foliation (S_m, 179 readings), (b) stretching lineation (L_{st}, 115 readings), (c) fold axes of early upright folds (FA 1, 34 readings), and (d) fold axes of later drag folds (FA 2, 15 readings).

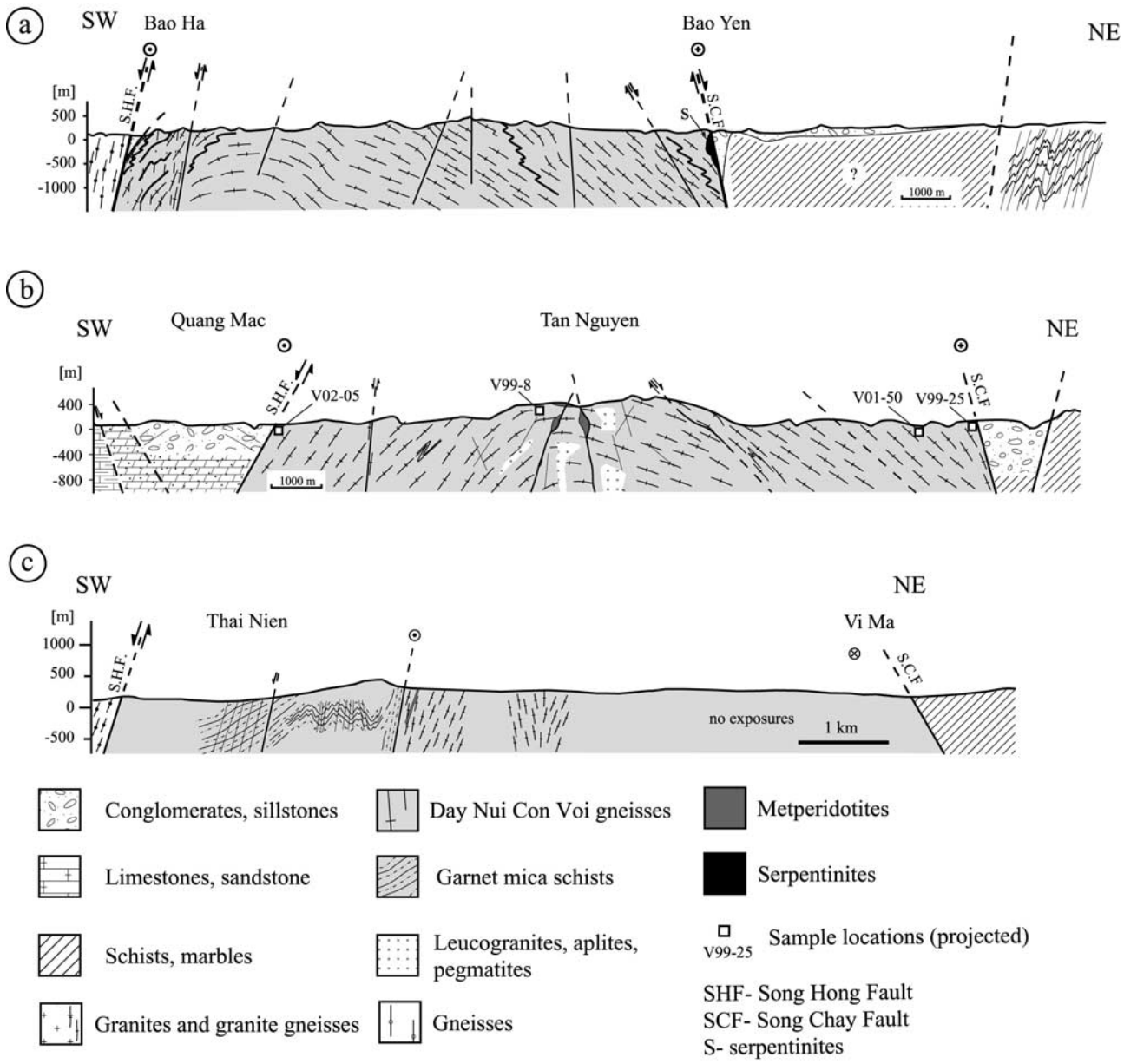

Figure 3. Cross sections. See Figure 2 for locations.

in the Bao Yen–Bao Ha section (Figure 3a) or some 40 km NW of Bao Yen (Figure 2a). They often occur in association with brittle faults with the same normal kinematics. In the vicinity of Bao Ha, the superposition of early symmetric, upright folds with these later, asymmetric "drag"-type folds was observed (Figures 5h and 5i).

[15] Moderately dipping normal faults, oriented at an acute angle relative to the trend of the RRSZ, are locally found. A typical example was documented in the vicinity of the SH fault close to Thai Nien (Figure 3c), where the main foliation in the garnet mica schists is oriented E–W and dips south. Downdip stretching lineations together with a pervasive extensional crenulation cleavage point to normal movement (Figures 6a and 6b).

3.1.2. Deformation in the Core of the DNCV Antiform

[16] The central part of the DNCV massif shows a different deformation style. The core of the antiform is formed by high-grade, highly deformed and migmatitic gneisses with a gently to moderately dipping foliation (Figures 6c–6f) and a well-defined NW–SE trending stretching lineation on the main, high-temperature foliation planes. The trend of this lineation is parallel to the strike-slip-related lineation in the limbs of the dome described above. However, unlike the SH and SC fault zones, kinematic indicators linked to this lineation are very scarce and difficult to interpret. This is due to the strong attenuation and tectonic disruption of the core of the antiform and lack of good quality exposures. The gneissic fabric is often cut

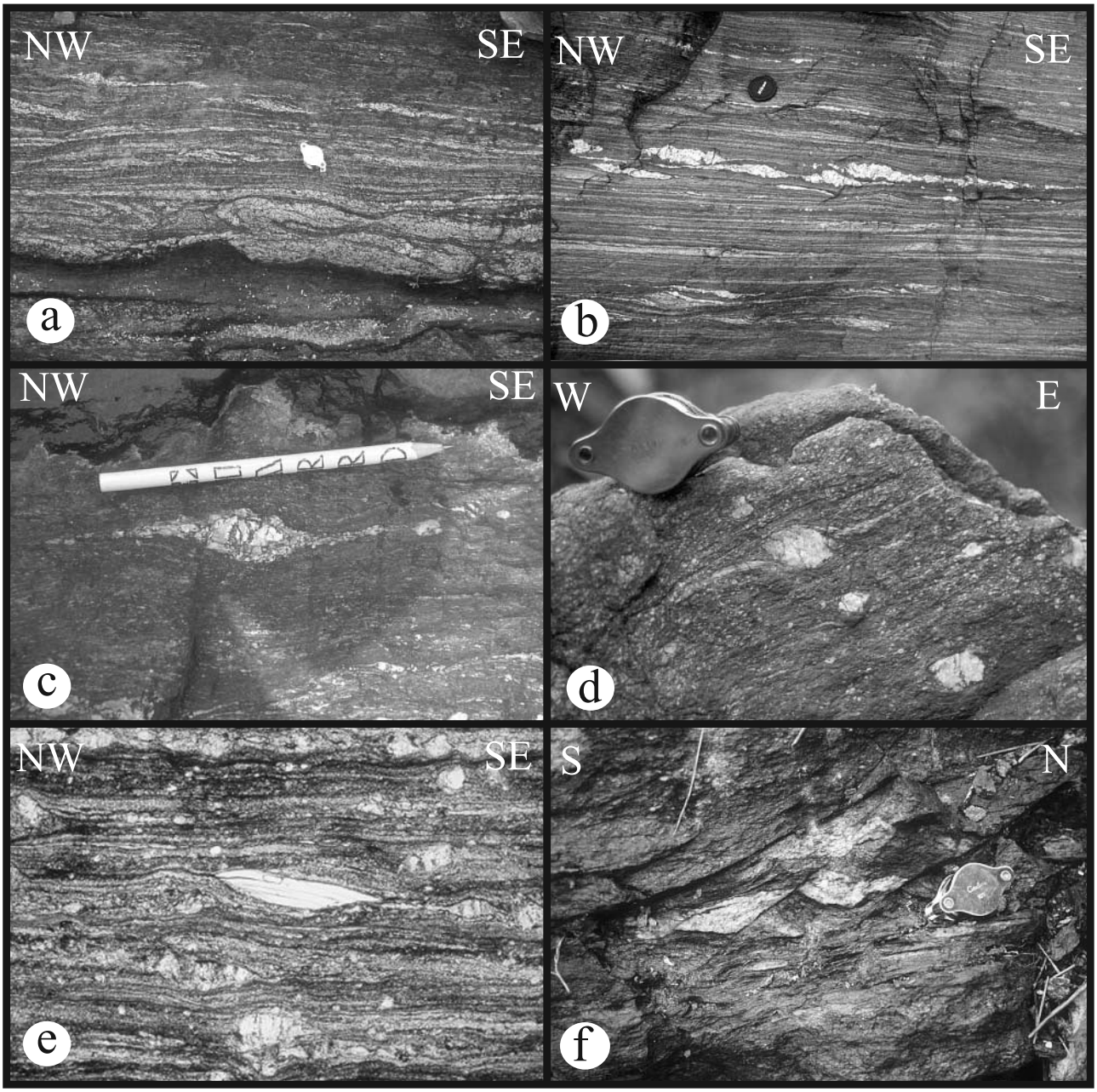

Figure 4. Examples of typical rock textures and sinistral kinematic indicators in the DNCV massif. (a) Minor fold vergence and sinistral shear bands, (b) sinistral shear band (lower part of the photograph) and stretched asymmetric feldspar clasts, (c) sigma clast, (d) delta clast, (e) mica fish, (f) brittle shear bands.

by vertical to moderately dipping normal faults (Figures 6c and 6f).

[17] Throughout the entire core of the DNCV massif there is widespread evidence for a very high degree of crustal melting expressed by numerous intrusions of mainly leucogranites, quartz veins, and aplites (Figures 6c and 6f). The largest amount of melt is observed in the core of the antiform, where the proportion of melt and gneisses are comparable. Numerous leucogranitic bodies were deformed together with their host rocks since the earliest stage. Others

Figure 5. (a) Early upright fold in gneisses. (b) SW verging drag folds and (c) sigma clast indicating top-to-SW movement from the Bao Ha area. (d–g) Examples of drag folds with subhorizontal axial planes. (h–i) Fold superposition pattern of early upright folds F1 refolded by drag folds F2. See text for details and Table S1 for GPS coordinates of each outcrop.

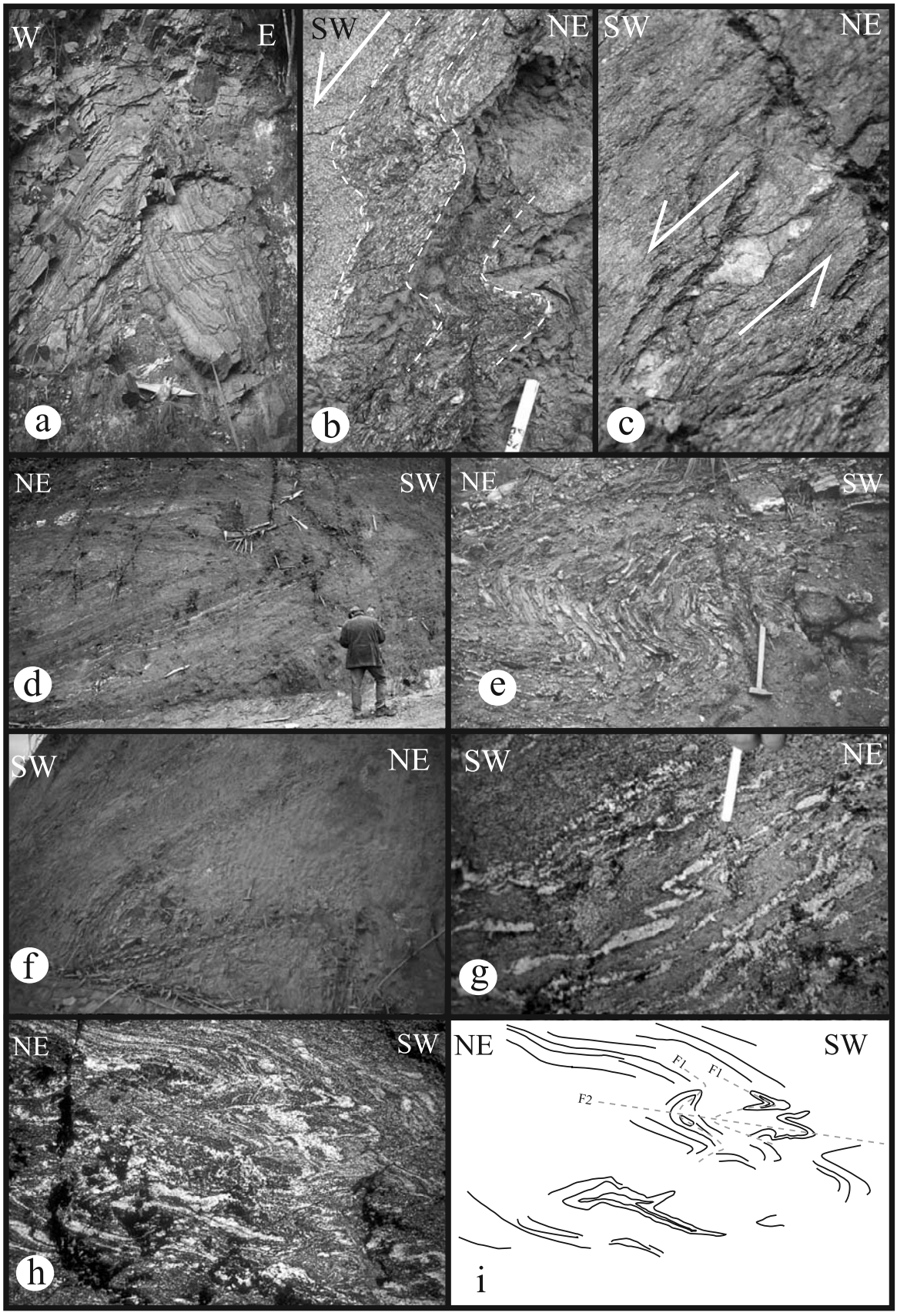

Figure 5

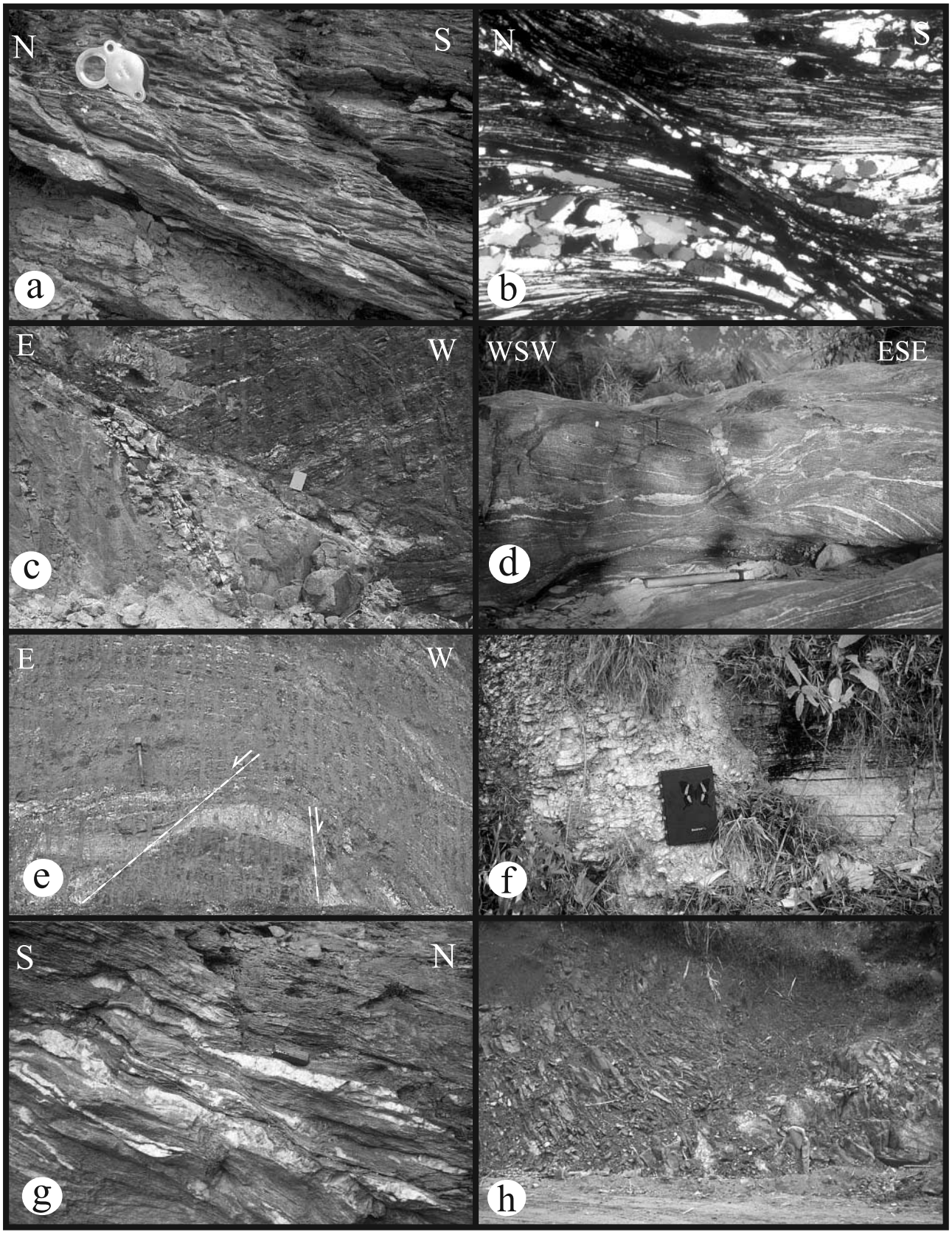

Figure 6

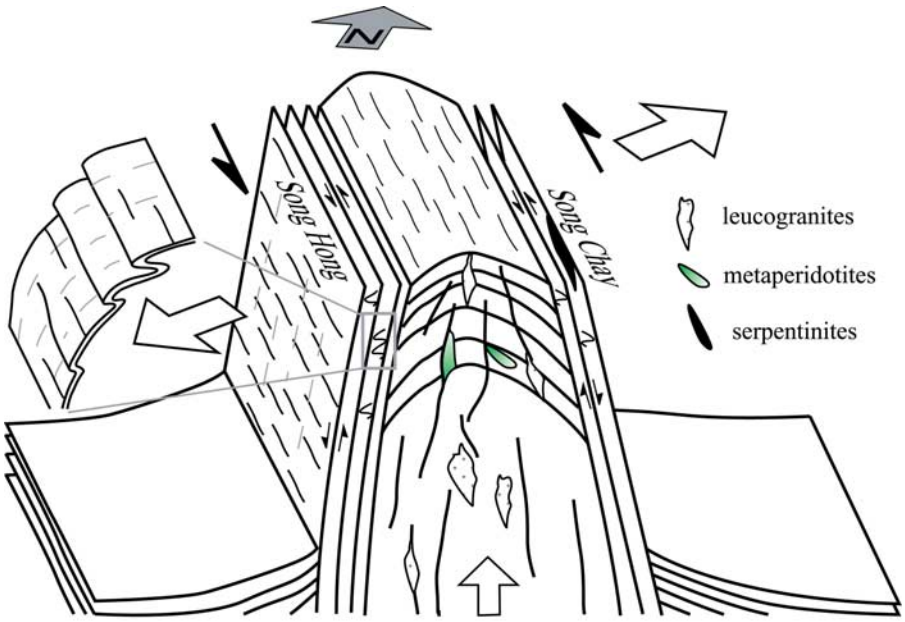

Figure 7. Structural model for the Day Nui Con Voi massif. Uplifted and exhumed, previously deformed and metamorphosed middle crust, strongly reworked along the margins by strike-slip and extensional shear with drag-type folds developing in the Song Hong and Song Chay fault zones. Note the different structural positions of serpentinites and metaperidotites (see text for details). White arrows mark the NE–SW regional extension direction.

are practically undeformed or, at most, show some late brittle deformation, indicating that melt production outlasted the ductile deformation phase.

3.2. Kinematic Interpretation

[18] As discussed above, the dominant structural characteristics of the RRSZ rocks is the pervasive sinistral shearing recorded predominantly along the margins of the DNCV antiform (Figure 7). During this deformation phase, symmetric, upright folds formed and folded the DNCV mylonitic fabric. We interpret these folds as resulting from the local shortening component within a broad sinistral shear corridor and the progressive rotation of the fold axes toward the flow direction. Numerous small-scale normal faults oriented at an acute angle to the trend of the belt are consistent with the left-lateral shear, and hence are interpreted as a consequence of the local stretching vector within the same wrench corridor. Extension caused the opening of relatively small pull-apart basins, which are filled with Neogene deposits [e.g., *Wysocka and Świerczewska*, 2003]. We stress that this type of extension is only a local phenomenon and should not be confused with the downdip shearing documented along the SH and SC faults that reflects regional NE–SW extension.

[19] Asymmetric SW and NE verging folds with NW and SE subhorizontal to gently plunging axes in the vicinity of the SH and SC faults are interpreted as due to downdip dragging of the preexisting foliation on the edges of the DNCV massif during the formation of the large-scale antiform and its exhumation (Figure 7). The same downdip tectonics along the SH and SC faults is deduced from kinematic indicators like quartz sigma clasts (Figure 5c) or quartz fabric (see below). The common association of these folds with synthetic brittle normal faults, whose kinematics point to the same extensional direction, suggests that a transition from ductile to brittle conditions occurred during the SH- and SC-driven exhumation of the DNCV antiform (Figure 7). We interpret these extensional fabrics as resulting from major downdip shearing along the opposite verging SH and SC faults, which bound the DNCV massif. Similarly oriented extensional fabrics were also observed outside the DNCV shear zone, within the low-grade metasediments near Bac Ha in the Song Chay dome area (Figure 6g). Minor fold vergence and extensional shear bands again point to a NE–SW oriented extension direction.

Figure 6. (a–b) Top-to-south extensional crenulation cleavage in garnet mica schists. (c) Brittle normal fault and (d) subhorizontal foliation in the core of the DNCV massif. (e) A pair of small-scale conjugate, brittle normal faults resembles the overall large-scale structure of the Day Nui Con Voi (see text for details). (f) Early leucocratic dike cut by the horizontal foliation present in the neighboring gneisses. (g) Top-to-north extensional shear bands in the Bac Ha area. (h) Exposure of deformed metaperidotites in the Tan Nguyên area. See text for details and Table S1 for GPS coordinates of each outcrop.

[20] These drag-type folds could alternatively be interpreted as a-type folds of *Malavieille* [1987]. In the studied case, however, this interpretation is not plausible. First, a-type folds should appear across the entire massif instead of being confined exclusively to the fault zones. Secondly, if they truly were a-type folds formed during left-lateral shearing, there should not occur a systematic set of lineations oriented at high angle relative to their fold axis. Finally, the kinematic significance of these folds is confirmed by the consistency of the shear direction deduced using their vergence with the shear direction established independently by other kinematic indicators such as rotated clasts and asymmetric microfabrics (section 4.2.2).

[21] The superposition of the early upright folds with these later, extension-related drag-type folds described above (Figures 5h and 5i) could not have originated from continuous progressive deformation. Instead, it indicates that, at least locally, extensional movements followed and overprinted strike-slip fabrics. This is in accord with the microstructural observations presented below.

4. Conditions of Shearing

[22] Although the strike-slip kinematics of the RRSZ is well documented [e.g., *Tapponnier et al.*, 1990; *Leloup et al.*, 1995; *Jolivet et al.*, 2001], metamorphic conditions of shearing remain controversial. *Leloup et al.* [2001] estimated that sinistral shearing occurred under high-temperature amphibolite facies conditions (>700°C) and propagated down into greenschist facies conditions. On the other hand, *Jolivet et al.* [2001] reported two distinct deformation stages, spatially confined to specific structural levels, with different deformation regimes partitioned between the limbs of the antiform and its core. They described amphibolite facies shearing exclusively in the core of the antiform, which was interpreted as a preexisting subhorizontal detachment above which left-lateral shearing took place. According to this model, left-lateral shearing took place exclusively under greenschist facies conditions and only along the margins of the antiform.

[23] In contrast to the latter interpretation, based both on PT estimates and microstructural investigations, we document high-temperature (amphibolite facies) conditions for both strike-slip and extensional fabrics in the limbs of the DNCV antiform. Our results, however, do not support the left-lateral shearing conditions in excess of 700°C proposed by *Leloup et al.* [2001] (see below).

4.1. PT Estimates

[24] Samples selected for PT estimates were collected from the core and the margins of the massif in order to gain insights into the metamorphic conditions of these two distinct structural domains. Whereas sample V99-08 was collected in the core of the antiform in the Yen Bai area, sample V02-05 was collected from the SW margin of the antiform in the vicinity of Trai Hut (Figure 3b, see Table S1 for GPS coordinates). Both samples show the same peak metamorphic paragenesis garnet + biotite + sillimanite + K-feldspar + plagioclase + quartz. Small amounts of chlorite and muscovite formed during retrogression at the expense of garnet and feldspar. Common accessories are monazite, zircon, apatite and rarely rutile. Garnet and feldspars form porphyroclasts in finer grained matrix of quartz and biotite. Garnet is usually strongly flattened and has inclusions-rich cores composed dominantly of quartz, substantial amount of zircon, monazite and more rarely biotite.

[25] Mineral compositions used for PT estimates are presented in Table S2. Traverses along the longer axes of garnets show flat patterns across nearly the entire crystal except for the rims. Flat zonation patterns indicate that major elements were completely homogenized and the rims were equilibriated with the matrix minerals. Hence our estimates were conducted using the composition of the garnet rim and matrix minerals. Thermodynamic calculations were conducted for the peak metamorphic assemblage using Thermocalc [*Powell and Holland*, 1988] and gave $P = 0.56 \pm 0.15$ GPa at $T = 810 \pm 60$°C for sample V99-08 and $P = 0.70 \pm 0.16$ GPa at $T = 820 \pm 60$°C for sample V02-05 (Figure 8). Both samples recorded similar T conditions, close to the liquidus line for metapelites (Figure 8). This is in agreement with the regional observation that DNCV rocks locally underwent partial melting. Pressure estimates seem different at first but they strongly overlap within their errors and hence are statistically indistinguishable. Previously published PT estimates [*Nam et al.*, 1998; *Leloup et al.*, 2001] show the same pressure range but at somewhat lower temperatures (Figure 8). The observed differences in temperature are most likely due to the use of different calibrations and/or sample selections. We were unable to determine the PT conditions for the retrograde phase due to unsuitable mineral paragenesis. Quantitative observations were provided by *Nam et al.* [1998], who determined greenschist facies conditions as ~480°C at 0.3 GPa.

[26] On the whole, geothermobarometric estimates for samples from various locations within the DNCV in this and other studies, point to rather similar peak PT conditions across the whole massif at about 700–800°C and 0.5 to 0.9 GPa (Figure 8).

[27] *Leloup et al.* [2001] used this type of thermodynamic PT estimates as evidence for sinistral shearing conditions in DNCV rocks in excess of 700°C. Such high-temperature conditions are based on the interpretation of the peak metamorphic paragenesis as synkinematic with respect to sinistral shearing. We did not find unequivocal proof in favor of this interpretation. On the contrary, our microstructural observations point to diffuse prekinematic garnet growth (we treat this topic in more details while presenting the conditions of sinistral shearing), and consequently we do not link our geothermobarometric estimates to the dynamic left-lateral shearing conditions, whose estimates we present in sections 4.2 and 4.3.

4.2. Microstructural Analysis

4.2.1. Left-Lateral Shear Conditions

[28] The main metamorphic paragenesis that records sinistral kinematics and formed under amphibolite facies conditions is given by biotite, sillimanite, plagioclase, K-feldspar and quartz. All minerals are strongly elongated

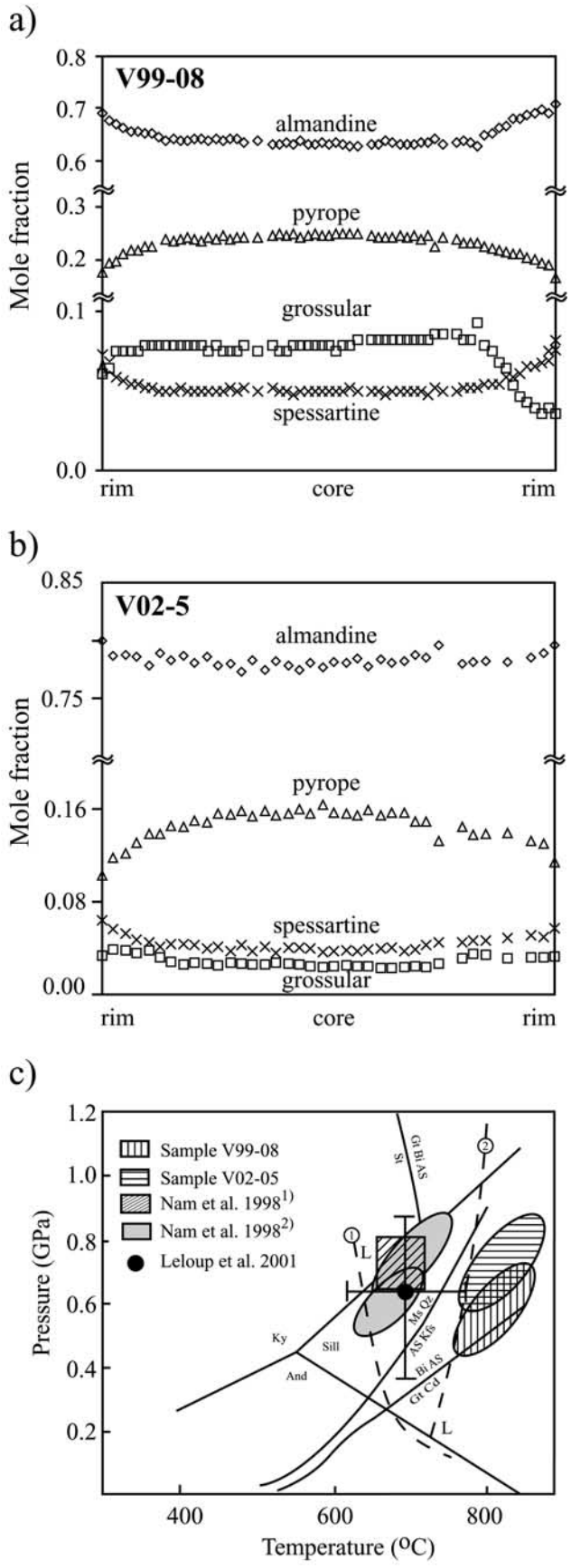

and flattened (Figure 9a). Garnets have a grain size up to several centimeters and often occur as porphyroclasts. They generally have a very strong shape preferred orientation, with the long axes parallel to the stretching lineation. Garnet aspect ratios reach values up to 4:1 (Figure 9d). Several features, such as dumb-bell-shaped crystals and strongly stretched and lensoid shaped grains, indicate their plastic deformation. Garnet crystals are always fractured and tension gashes are oriented consistently with the extension direction imposed by the sinistral kinematics that dominates the SH and SC faults mylonites (Figure 9d). The fracturing process clearly postdated the ductile deformation of garnets but is still coeval with the bulk high-temperature sinistral deformation phase. Garnets are locally cut across and displaced along shear planes, as also observed by *Leloup et al.* [2001]. All garnet features described above, together with the observation that the regional foliation always flows around garnets, wrapping them around, suggest the prekinematic nature of garnets with respect to sinistral shearing and to the regional foliation-forming event.

[29] In garnet or plagioclase pressure shadows and in sinistral S/C'shear band planes, sillimanite with biotite form a stable paragenesis (Figures 9b and 9c). This constrains left-lateral shearing temperatures within the sillimanite stability field.

[30] Similar to garnet, plagioclase is generally prekinematic (Figure 9e). Plagioclase is characterized by undulose extinction, deformation lamellae and bands, kink bands as well as core-mantle structures with dynamically recrystallized rims (Figure 9f). The size of the recrystallized grains ranges between 20 and 80 μm. Grain boundaries are often serrated from the migration of the boundaries themselves (Figure 9g). The bulges have a similar grain size as the subgrains, suggesting that the new grains have formed by a combination of subgrain rotation and local grain boundary migration by bulging recrystallization. In some samples, feldspar is recrystallized almost completely (Figure 9h). The microstructural features described above imply deformation temperatures on the order of 500–550°C [e.g., *Vernon*, 1975; *Simpson*, 1985; *Vernon and Flood*, 1988], well below the T estimates for the peak metamorphism.

[31] Further support in this direction comes from quartz microstructures and quartz fabric analysis, which confirm a stage of high temperature (>500°C, but lower than 700°C) during sinistral shearing affecting the steep margins of the large-scale DNCV antiform. Almost pure quartz veins were sampled at the margins of the DNCV massif and were

Figure 8. Rim-to-rim major element zonation patterns in garnet from samples (a) V99-08 and (b) V02-05. (c) Simplified PT diagram with geothermobarometric estimates from this and previous studies. See text for details. Nam et al. 1, amphibolite; and 2, metapelite; AS, aluminosilicate; And, andalusite; Cd, cordierite; Gt, garnet; Kfs, K-feldspar; Ky, kyanite; L, liquid; Ms, muscovite; Pl, plagioclase; Sill, sillimanite. Reactions (1) pelite-saturated solidus after *Thomson* [1982] and (2) liquidus line after *Le Breton and Thompson* [1988].

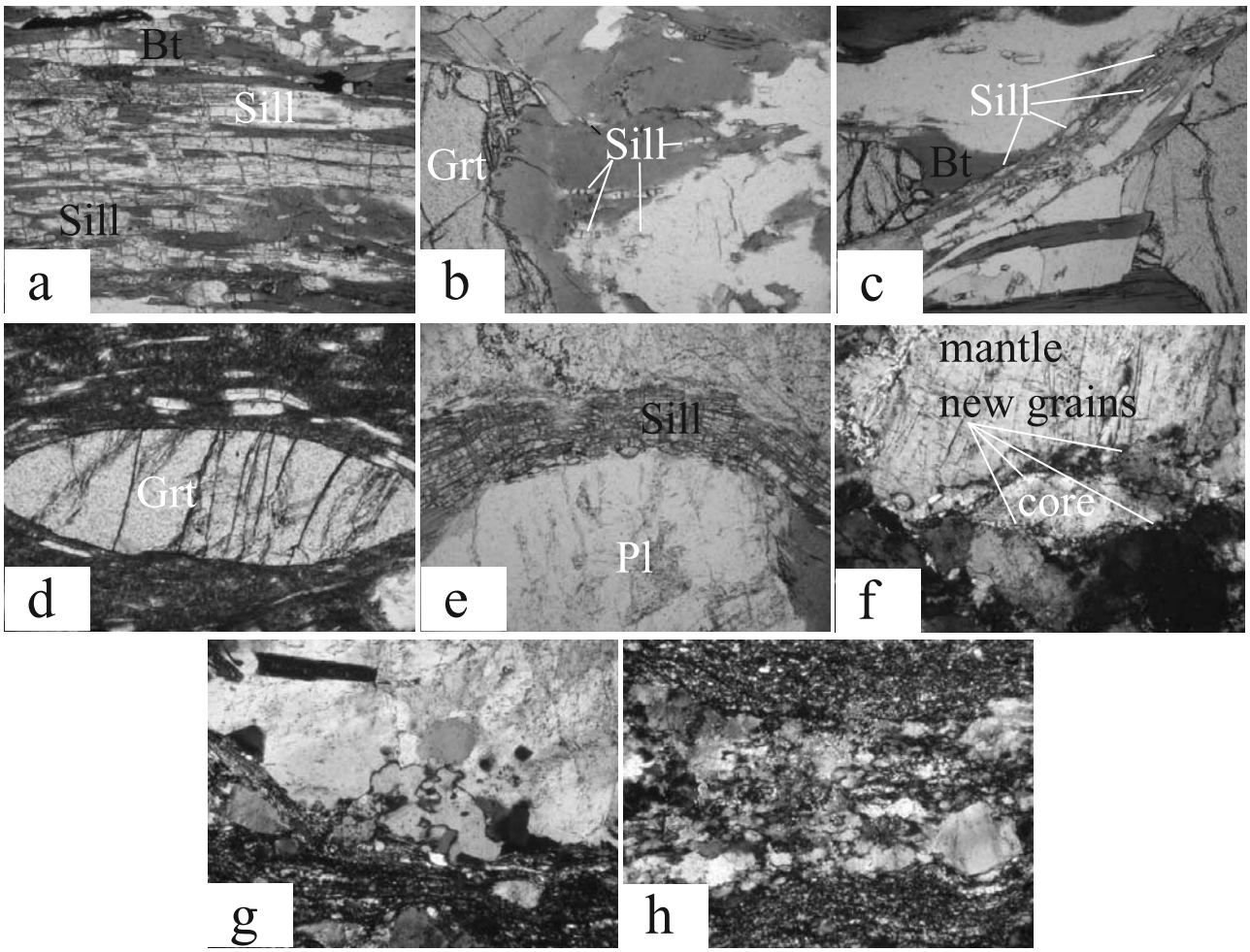

Figure 9. Examples of the dominant paragenesis in the DNCV paragneisses and examples of plagioclase microstructures. (a) DNCV regional foliation defined by prismatic sillimanite crystals and red biotite. (b) Prismatic sillimanite crystals in a garnet pressure shadow. (c) Prismatic sillimanite crystals aligned along a shear band plane. Shearing took place in the sillimanite stability field. (d) Highly stretched and flattened garnet within the regional foliation. Tension gashes are oriented consistently with the sinistral kinematics of the Red River shear zone. (e) Plagioclase (when not completely recrystallized) is prekinematic. A sillimanite crystal of the regional foliation forming paragenesis is bent around a plagioclase clast. (f) Core-mantle structure developed at the edge of a dynamically recrystallized plagioclase. (g) Example of serrated grain boundary with evident bulging recrystallization. (h) Completely recrystallized plagioclase layer. No porphyroclast relics are left.

studied in thin sections. The vast majority of quartz samples show evidence for a very strong, complete dynamic recrystallization. Two representative samples from the limbs of the DNCV massif (01/50 and 99/26) were chosen for quartz fabric measurements. The results are summarized below and shown in Figure 10.

[32] Specimen 01/50 (see Table S1 for GPS coordinates) was collected along the eastern boundary of the DNCV complex, not more than 200 m away from the Song Chai River. It is an almost pure monomineralic quartz vein parallel to the foliation. The optical microstructure is characterized by a mylonitic foliation defined by thin mica crystals (Figure 10a) aligned parallel to the regional foliation and lenses of strongly sheared clasts of intensely recrystallized plagioclase, mostly by subgrain rotation (Figure 10b). Plagioclase clasts display asymmetric pressure shadows marked by white mica crystals. Sense of shear is sinistral and agrees with the bulk sinistral oblique quartz fabric. Plagioclase clasts generally lack fractures although some of them display tension gashes oriented at about 90° to the direction of the extensional axis of the incremental strain ellipsoid.

[33] Quartz is dynamically recrystallized by bulging and grain boundary migration processes. Grain boundaries are very irregular and crystals display very complex geometries and shapes. However, locally a weak shape fabric is recognizable (S_b in Figure 10a). The latter is mostly due to slightly elongate grains and asymmetric grain boundary

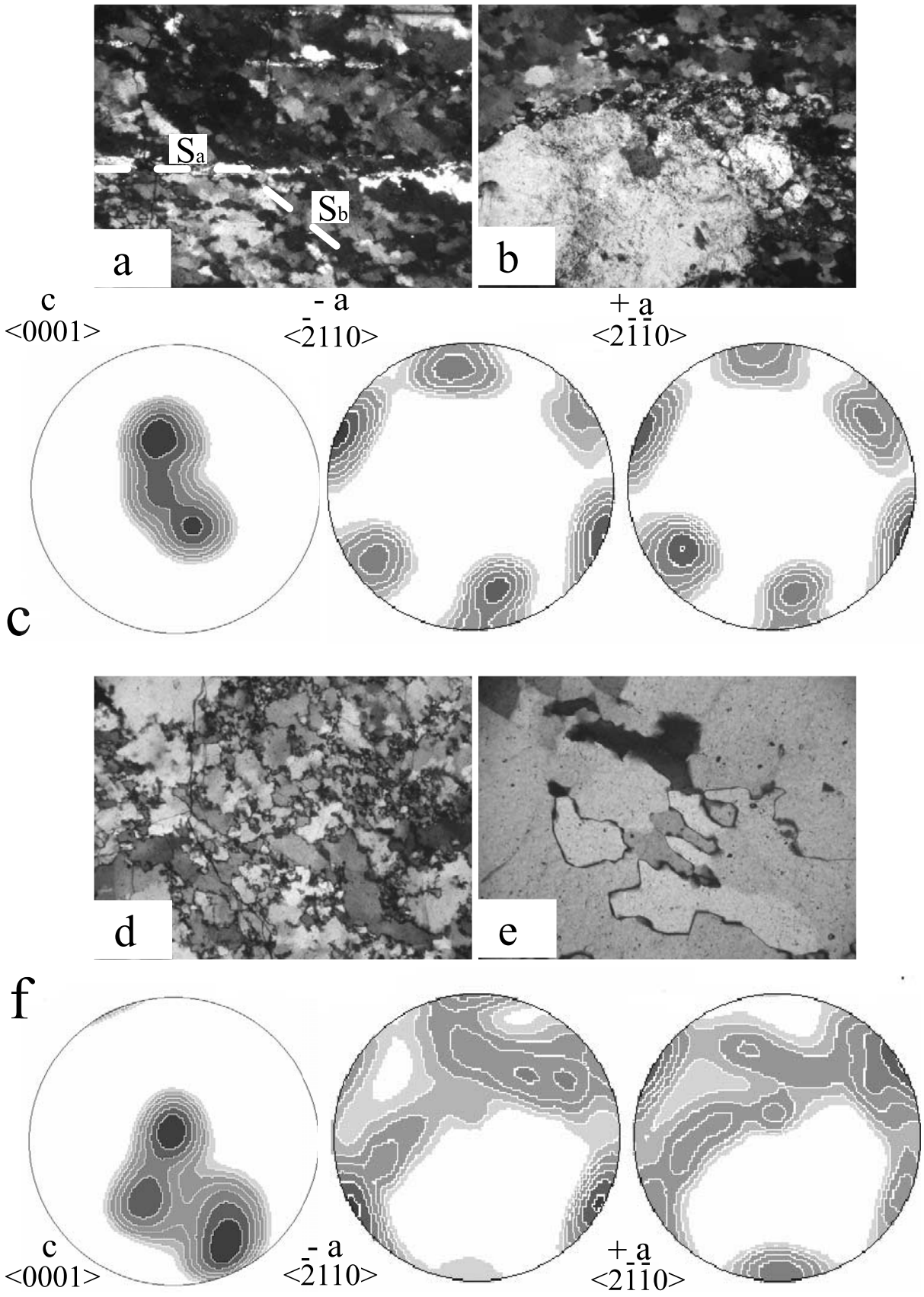

Figure 10

bulges. Intracrystalline deformation is recognizable in deformation bands and in widespread undulose extinction. Shear bands are absent from the quartz vein whereas they are strongly developed (with a sinistral kinematics) in the more micaceous matrix adjoining the quartz vein but disappear within the first millimeter or so of the contact. On the basis of these microstructural features a deformation temperature in the amphibolite facies of at least 500–550°C is inferred [e.g., *Schmid and Casey*, 1986; *Mainprice et al.*, 1986; *Law*, 1990; *Stipp et al.*, 2002].

[34] Results of quartz texture goniometry crystal preferred orientation (CPO) measurements for the c, $-\langle a\rangle$ and $+\langle a\rangle$ axes are displayed in the pole figures of Figure 10c. The bulk texture shows a c axis cluster with two submaxima parallel to the intermediate strain axis Y with a marked tendency to spread along the YZ plane. Along the primitive circle there are three a axis maxima, suggesting a ''single-crystal'' orientation, with the a axis maxima asymmetrically disposed about the macroscopic fabric axes.

[35] Sample 99/25 (see Table S1 for GPS coordinates) is a thin quartz vein found in strongly sheared micaceous gneiss. It was collected from the eastern margin of the DNCV in the vicinity of Bao Yen. Quartz is almost completely dynamically recrystallized by grain boundary migration (Figures 10d and 10e). Few plagioclase porphyroblasts are scattered in the quartz-defined schistosity. Plagioclase is ductilely deformed and locally defines sinistral mantle-sigma clasts with asymmetric wings formed by recrystallized plagioclase. Quartz grain boundaries are lobate and grain contacts are interfingering (Figure 10e). Locally, as in the case of sample 01/50, grains display large sizes and irregular ameboid shapes to such an extent that it becomes difficult to recognize and define individual grains. Grains are internally strained and display evidence of undulose extinction, deformation lamellae and bands. Texture analysis results are very similar to those of sample 01/50 (Figure 10f). The c axis pole figure shows a relatively diffuse maximum spread around the intermediate strain axis Y. The fact that an important C axis cluster is still present along the primitive circle points to a probable fabric transitional character between a crossed girdle distribution and a single, sharp maximum centered on the Y axis.

[36] The pattern obtained is generally attributed to quartz dislocation creep phenomena on the prism planes in the $\langle a\rangle$ direction, which is supposedly mainly active under amphibolite-facies conditions [e.g., *Tullis*, 1977; *Schmid and Casey*, 1986; *Mainprice et al.*, 1986; *Law*, 1990]. A crucial upper temperature limit is provided by the absence in the measured samples of prism $\langle c\rangle$ slip (reported instead by *Leloup and Kienast* [1993], for a sample from the Ailao Shan complex), which limits the temperature of deformation to below the granitic solidus (about 700°C [e.g., *Kruhl*, 1996]). A lower temperature limit is provided by the pervasive dynamic recrystallization of feldspar in the studied mylonites, which indicates temperatures higher than 500–550°C, as noted above.

4.2.2. Extensional Shear Conditions

[37] Structures and microstructures of tectonites representative of the DNCV extensional deformation phase cover a large variety of shearing conditions. The onset of normal faulting along steep fault planes began still under high-temperature conditions corresponding to a fully ductile environment. Massive amphibolites and amphibolite facies fabrics are sheared and synkinematically folded consistently with extensional shearing and show drag folds with axes perpendicular to the downdip stretching direction. Quartz-plagioclase mylonites sampled within the steep downdip faults show evidence of plagioclase dynamic recrystallization and quartz grain boundary migration processes, very similar to the microstructural features discussed above for the plagioclase-rich mylonites directly linked to the earlier high-temperature sinistral strike-slip shearing.

[38] Similar to the strike-slip fabrics, extensional structures had a prolonged activity along a retrograde path and extensive evidence of the same deformation phase is found preserved under greenschist facies conditions down to pure brittle structures. Microstructural evidence shows an intense reworking of the earlier strike-slip higher-temperature fabric. Rocks present a remarkable reduction in the grain size of the constituent minerals, like mica (Figure 11a) and sillimanite (Figure 11b). Bands deformed by brittle cataclastic flow are common (Figure 11c) and there is abundance of hydraulic fractures at all scales. Clasts are very irregular in shape, angular and poorly sorted, which indicates high strain rates and/or high fluid pressure.

5. Structural Position, Petrography, and Metamorphism of the Ultramafic Rocks

[39] Ultramafic rocks in the DNCV massif are very rare. Two very well known locations of strongly serpentinized ultramafic rocks are situated near Bao Yen, along the eastern margin of the DNCV (Figure 2). Another exposure is found along a relatively new road cut presented in cross section C in Figure 3. Because these rocks potentially bear a record of processes happening at greater depths than the surrounding

Figure 10. Microstructural features of quartz in samples (a and b) V01-50 and (d and e) V99-25. (c–f) Pole figures for the c, $-\langle a\rangle$, and $+\langle a\rangle$ axes for sample V01-50 and V99-25, respectively. The pole figures are oriented with the X-Y foliation plane perpendicular to the page and oriented east–west and the stretching lineation direction horizontal and plunging to the left. In Figure 10a the regional mylonitic foliation is marked by thin mica crystals, here visible as white small E–W aligned crystals (Sa). A weak oblique shape fabric Sb is defined by slightly elongate grains and asymmetric grain boundary bulges. The quartz mylonite is completely recrystallized by grain boundary migration. In Figure 10b, core-mantle structure developed at the edge of a dynamically recrystallized plagioclase within a dynamically recrystallized quartz mylonite. In Figure 10d, tectonite V99-25, displaying intense dynamic recrystallization by grain boundary migration. In Figure 10e, detail of the previous microstructure is shown. Note the serrated, high-mobility grain boundaries.

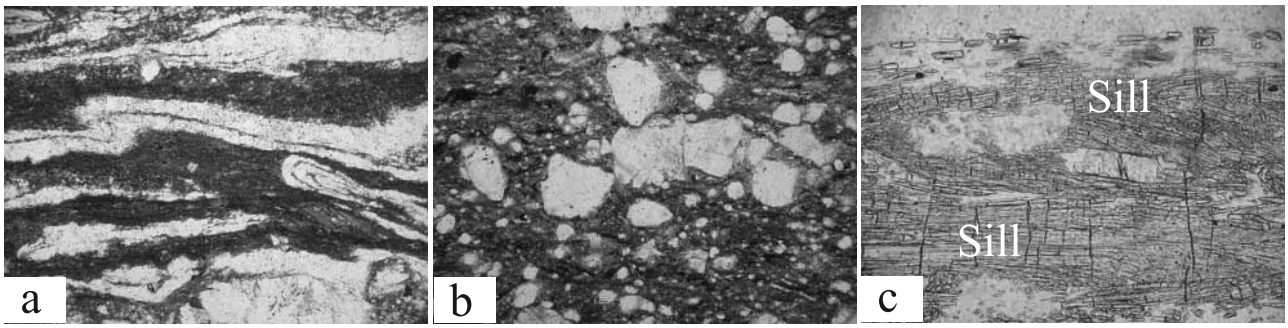

Figure 11. Examples of microstructures associated with the steep, normal faulting along the edges of the DNCV massif. (a) Ductile features (asymmetric folds showing top-to-the-SW kinematics) associated with the steep normal Song Hong fault (Bao Ha area). Note the extremely fine grain size of biotite. (b) Cataclastic flow processes have created a series of poorly sorted angular clasts. One of the parent grains is still recognizable in the center of the microphotograph, whose mechanical disruption under high strain rate and/or high fluid pressure conditions has generated the small irregular clasts (Bao Ha area). (c) Fine-grained sillimanite crystals resulting from mechanical grinding of larger, prismatic grains.

gneisses, below we provide their brief characterization along with initial petrogenetic studies.

5.1. Serpentinites From Bao Yen

[40] Serpentinites from the vicinity of Bao Yen are found within the Song Chay fault zone, caught between DNCV gneisses to the west and low-grade carbonates to the east (Figures 2 and 3c). They are massive, composed of serpentine group minerals, chlorite, diopside and magnetite (Figure 12a), which points to greenschist-facies metamorphism [*Ulmer and Trommsdorff*, 1999]. An $\varepsilon_{Nd(CHUR)}$ of 7.5 was obtained, which is the same as for the basalts of the South China Sea [*Nguyen et al.*, 1996, and references therein], suggesting a similar asthenospheric source. A very high $\varepsilon_{Hf(CHUR)}$ of 29.4 confirms their asthenospheric origin (Table S3).

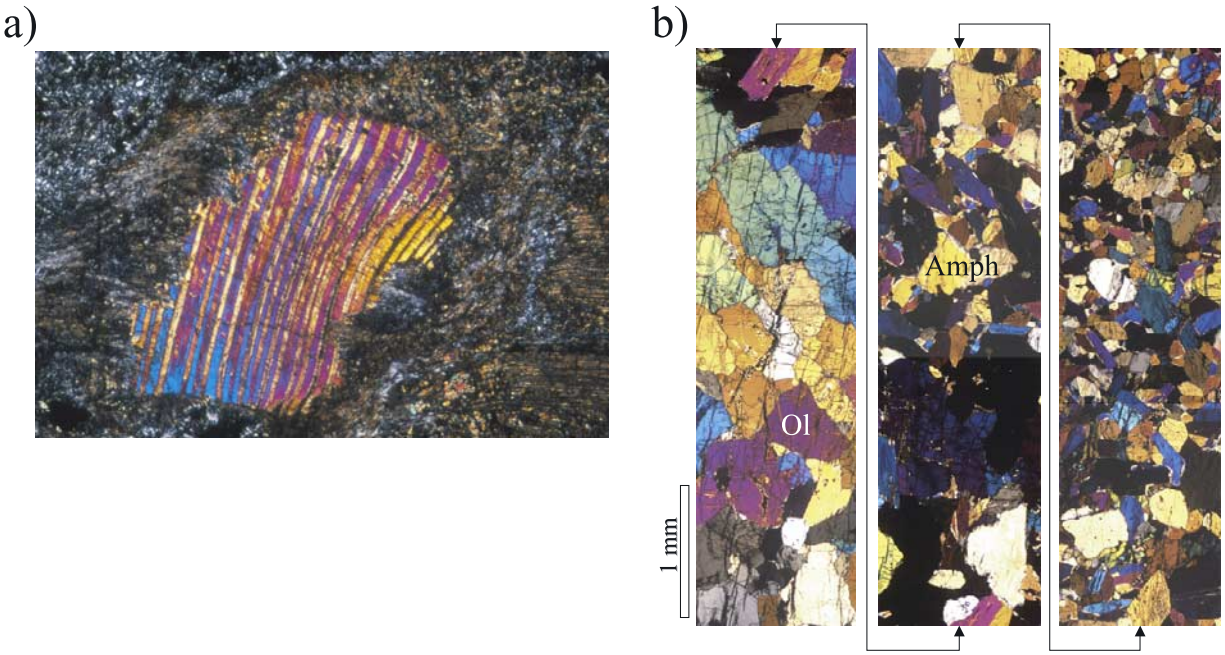

Figure 12. (a) Serpentinite from the Bao Ha region. Relics of pyroxene in a strongly serpentinized matrix. (b) Ultramafic rocks from the central part of the DNCV (Tan Nguyên area, see Appendix A for GPS coordinates), consisting of olivine, hornblende, spinel, and minor orthopyroxene. Note the coarser olivine layers in the lower part gradually passing into finer, amphibole-rich layers. Arrows indicate the continuity of the photographs. Ol, olivine; Amph, amphibole. The amphibole-rich layer probably represents a former pyroxenite, while the olivine-rich layers represent a mantle peridotite.

5.2. Metaperidotites From Tan Nguyên Area

[41] Metaperidotites along the Tan Nguyên section, about 20 km SE of Trai Hut, reveal a completely different structural setting and petrogenesis (see Table S1 for outcrop coordinates). They are situated directly in the core of the DNCV antiform and are only slightly serpentinized (Figure 6h). They seem to be associated with steeply dipping to subvertical faults and contain xenoliths of the surrounding gneisses. The metaperidotites are composed dominantly of Mg-hornblende, olivine, brown-green spinel, orthopyroxene, and minor chlorite and magnetite (Figure 12b). Phlogopite (partially chloritized), apatite and Ni sulphides occur as accessory minerals. Olivine forms a tabular polygonal mosaic and is in textural equilibrium with Mg-hornblende, orthopyroxene and spinel. Numerous spinel inclusions are found in Mg-hornblende and orthopyroxene. Olivine is composed of 82% forsterite, amphibole is classified as Mg-hornblende with up to 6.5 wt % Al_2O_3 and Mg # of ~0.88 to 0.9. Spinel is Al-rich and strongly zoned with Cr-rich cores and Al-rich rims. Cr number varies between 0.05 and 0.20 (Table S4). Chlorite is close to a clinochlor composition, with Mg # of about 0.91. Green spinel (Al-rich) is preferentially found in hornblende-rich layers, while in olivine-rich layers, the color is more brownish, indicating higher Cr content in the olivine-rich part. This suggests the layered nature of the protolith. Coarser layers are dominated by olivine while finer layers are amphibole-rich (Figure 12b). The five-phase assemblage in the ultramafic rocks (ol+opx+Mg-hbl+spl+chl) is characteristic of metaperidotites equilibrated under upper amphibolite facies conditions [*Trommsdorff and Evans*, 1974]. The observed mineral reactions and paragenesis allow determination of the temperature of metamorphism undergone by these rocks. The ol+en+Mg-hbl+spl±chl paragenesis and the Al zoning in spinel indicate the prograde breakdown reaction of Mg-chlorite. In this continuous reaction, spinel is progressively enriched in Al and forms together with olivine and orthopyroxene. The few relics of chlorite indicate that the reaction went nearly to completion. For the pure MASH system, the breakdown of chlorite to olivine, orthopyroxene and spinel occurs at about 780 to 800°C in the pressure range of 0.5 to 0.8 GPa [*Jenkins and Chernosky*, 1986]. However, in a natural system, spinel will form at lower temperatures, due to preferred incorporation of Cr and Fe^{3+} in spinel compared to chlorite [*Evans and Frost*, 1975]. In addition, whole rocks and minerals from the metaperidotites described from the RRSZ (Table 2) have somewhat lower Mg # than similar metaperidotites [*Katzir et al.*, 1999]. Thus, for a pressure of about 0.8 GPa derived from the surrounding sillimanite gneisses [*Nam et al.*,1998; *Leloup et al.*, 2001; this study], temperature estimates of 700–750°C can be made. This is consistent with the absence of Mg-rich orthoamphibole in the metaperidotites, providing a minimum temperature estimate of about 700°C. On the other hand, clinopyroxene was not observed in the metaperidotites, limiting the upper temperature to about 800°C [*Ulmer and Trommsdorff*, 1999]. These temperatures overlap with temperature estimates for the host gneisses presented above.

[42] Initial isotopic studies, which estimate negative present-day $\varepsilon_{Nd(CHUR)}$ as −6.0 and −8.1, point to origin from an enriched lithospheric mantle source (Table S3). Equivalent $\varepsilon_{Hf(CHUR)}$ values of 2.4 and −2.2, respectively, are also low and seem to point to crustal contamination, which is most likely linked to metasomatic processes as indicated by the presence of phlogopite in both samples.

[43] Taking into account the low forsterite content in olivine, dominantly Al spinel composition, lack of clinopyroxene, and the layered nature of the rocks, as well as low ε_{Nd} and ε_{Hf} values, we interpret these rocks as representing metaperidotites (possibly pyroxenites) derived from a depleted mantle source and subsequently metasomatized by crustal fluids during amphibolite facies metamorphism.

6. Discussion

[44] The recognition of the DNCV antiform provided a critical argument to *Jolivet et al.* [2001] for interpreting the DNCV as an originally subhorizontal detachment, above which the retrograde transtensional RRSZ shearing developed [*Jolivet et al.*, 2001]. *Leloup et al.* [1995, 2001], on the other hand, did not favor the large-scale antiformal dome as a key structure of the DNCV massif, which they clearly expressed in their cross sections. The latter authors interpreted the flatness of the foliation in the antiform core as due to either the vertical flattening (kinematically linked to transtension) of an earlier, originally vertical foliation or as a relic of an earlier structure strongly reworked within the RRSZ. This interpretation is at odds to our observations, which clearly indicate that flat lying foliations in the core of the DNCV do not bear much record of RRSZ strike-slip reworking. Our study confirms that the DNCV massif forms a large-scale gneissic antiform with strongly reworked margins, a characteristic typical of core-complex type structures (Figure 7). The steep antiform limbs accommodated most of the transtensional and, locally, predominantly extensional movement. On the basis of the results presented above, we favor a much simpler interpretation of the observed changes in the orientation of the dominant foliation, according to which the antiform was formed in response to the uplift and exhumation of originally subhorizontal midcrustal gneisses within a transtensional crustal corridor (Figure 7).

[45] *Jolivet et al.* [2001] concluded furthermore that high-grade metamorphic conditions and the highest strain are present only in the core of the antiform (a denudated remnant of a midcrustal detachment). The edges of the DNCV massif, in their interpretation, would be reworked along steep faults only at a later stage, under retrograde greenschist facies conditions. The authors based their interpretation on the observation that sinistral kinematic indicators are always postsillimanite and contemporaneous with the crystallization of biotite, chlorite and muscovite, indicative of greenschist facies conditions. Our microstructural studies, however, show a different picture. We have documented amphibolite facies shearing (within sillimanite stability field) along the DNCV margins for both strike-slip and extensional structures. Moreover, regional observations

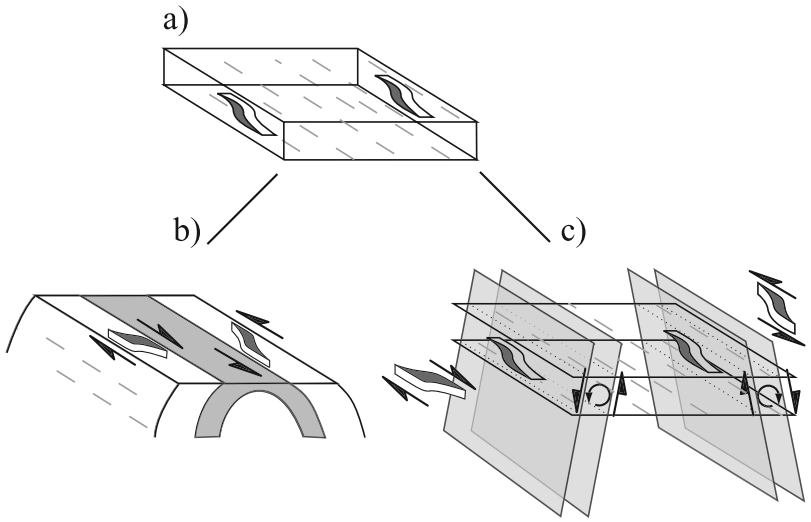

Figure 13. Rotation of kinematic indicators of an (a) originally horizontal layer due to either (b) folding or (c) shearing along opposite verging normal faults. In both cases, rotation leads to inverted, apparent left- and right-lateral sense of shear in the margins of the massif, which contradicts observations in the DNCV massif (see text for details).

show a strain gradient within the antiform, with the strongest high-temperature mylonitic fabric concentrated in the limbs, where the foliation attitude is very steep to subvertical. Deformation temperatures documented from the strike-slip and extensional structures were determined to be between 700 and 500°C. Temperature decreased into greenschist facies conditions only during the final phase of uplift and exhumation of the DNCV. We did not find evidence for shearing temperature above 700°C as reported by *Leloup et al.* [2001]. As mentioned above, such high-temperature conditions rely on the interpretation of garnet growth as synkinematic with sinistral shear and thermodynamic calculations, which indeed indicate temperature in excess of 700°C (see above). Since our microstructural observation support the interpretation of garnet crystallization conditions as prekinematic (relatively to sinistral shear), we do not directly link our thermobarometric estimates with the sinistral fabrics, which otherwise confirm metamorphic conditions in the temperature range estimated by *Leloup et al.* [2001].

[46] The possibility that the high-temperature strike-slip fabrics presented in this study in fact represent earlier flat-lying fabric passively rotated to their present subvertical position due to either folding or dragging in the footwall of the transtensional SH and SC faults, can be excluded. Folding around an axis parallel to the trend of the massif and of the regional stretching lineation would result in kinematic indicators showing opposite sense of shear in both limbs of the folds (Figures 13a and 13b). Similarly, passive rotation due to downdip movement and dragging along the opposite verging SH and SC faults would lead to the same kinematic inversion (Figures 13a and 13c). Because in both limbs of the DNCV antiform shear criteria are consistently left-lateral, we treat our temperature estimates as truly representative for sinistral strike-slip shearing conditions during RRSZ activity.

[47] Extensional fabrics within the RRSZ so far have been documented only for brittle conditions or invoked on the basis of fast cooling indicated by thermochronological studies [*Harrison et al.*, 1996; *Wang et al.*, 2000; *Leloup et al.*, 2001]. Whereas within the marginal part of the DNCV evidence for strike-slip movement is ubiquitous, dip-slip structures tend to be localized within rather narrow zones. Similar temperature conditions documented here for strike-slip and extensional structures suggest that both deformation regimes acted coevally, but were spatially localized into zones of more intense strike-slip or dip-slip shearing. Local obliteration of earlier strike-slip fabrics by extensional shear suggests period(s) during which extension dominated lateral slip. Kinematic analysis of the extensional fabrics in the DNCV and in the Song Chay dome area indicates a regional NE–SW extension direction, identical to that documented for the Bu-Khang area [*Jolivet et al.*, 1999; *Nagy et al.*, 2000]. All these studies support a major extensional phase in the region during Oligo-Miocene time.

[48] How and when the ultramafic rocks and high-grade gneisses were brought into contact, is open to speculation. Serpentinites from the Bao Yen area, unlike the adjacent DNCV gneisses, never experienced midcrustal conditions and recorded only greenschist facies metamorphism. Most likely these rocks represent a tectonic slice of oceanic lithosphere caught in the RRSZ. Metaperidotites observed in the core of the DNCV, on the other hand, could possibly indicate deep rooting of the RRSZ. This would imply that the RRSZ might have been able to penetrate through the "detachment" proposed by *Jolivet et al.* [2001] into the upper mantle. However, an alternative explanation is that the metaperidotites are remnants of an older history predating sinistral shear within the RRSZ. Indeed, the same high amphibolite facies conditions registered in the metaperidotites from Tan Nguyên and in the host sillimanite gneisses, may suggest that the metaperidotites were emplaced into the

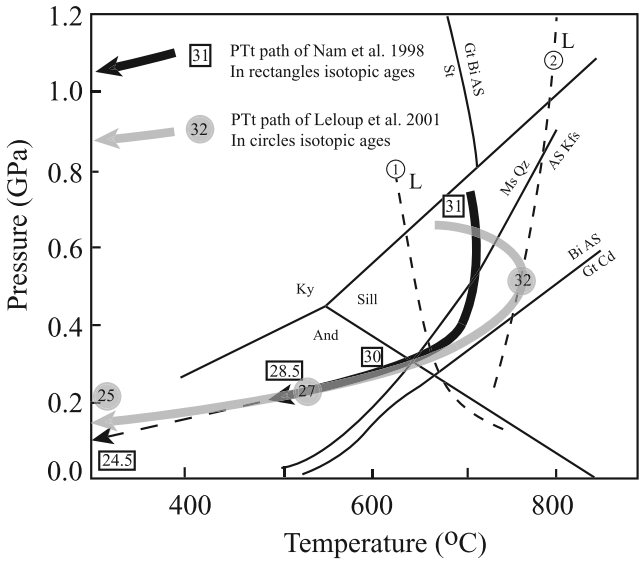

Figure 14. Pressure-temperature-time paths for the DNCV massif from *Nam et al.* [1998] and *Leloup et al.* [2001]. See text for details. Reactions are as in Figure 8.

middle crust and metamorphosed together with the host gneisses prior to the initiation of the RRSZ.

[49] The PT record in the DNCV massif requires ~20–25 km of exhumation [*Nam et al.*, 1998; *Leloup et al.*, 2001; this study]. So far, two uplift and exhumation mechanisms have been proposed for the DNCV massif. According to *Leloup et al.* [1995], oblique-slip combined with a very large amount of lateral displacement (700 ± 200 km) and some extensional component (in the case of the DNCV only) caused steady exhumation of the mid crustal gneisses produced as a result of shearing within a deeply rooted strike-slip shear zone. According to *Jolivet et al.* [2001], the RRSZ evolved instead from a single transpressive fault, the Song Chay fault. Subsequently, the Song Hong fault developed, facilitating the transition to a transtensional regime, which led to the exhumation of the DNCV. The normal component was mainly absorbed by the Song Chay fault.

[50] Our study indicates that both the SH and SC faults bear a record of an extensional event. Hence we propose that both faults played an equal role in accommodating the vertical movement of the DNCV massif. Below we propose a new scenario for the RRSZ evolution and for the exhumation of the DNCV rocks.

7. Tectonic Interpretation

[51] We present our tectonic interpretation in the three following steps:

7.1. Thinning of the Lithosphere

[52] Thinning of the lithosphere in SE Asia was postulated by *Chung et al.* [1997]. They investigated highly potassic magmas, which they interpreted as resulting from the removal of the basal continental lithosphere and subsequent heating by the upwelling asthenosphere. Ar-Ar and K-Ar dating of the potassic magmatism spans between 40 and 30 Ma, indicating that regional extension occurred at least since about 40 Ma. This timing finds further support in circa 40 Ma Sm-Nd garnet cooling ages obtained by *Anczkiewicz and Thirlwall* [2003] for the DNCV gneisses. Hot asthenosphere is the likely heat source for the metamorphism and melting of midcrustal and lower crustal rocks in northern Vietnam. This is an alternative to the synkinematic shear heating model proposed by *Leloup et al.* [1995], which has been shown to be problematic by *Gilley et al.* [2003]. The latter authors proposed instead large-scale heat advection due to large volumes of ascending magma as an alternative heat source. In the case of such interpretation, however, a mechanism generating such voluminous magmas is required. In our view, the upwelling of the asthenosphere due to lithospheric thinning could be a very plausible mechanism explaining both the high-temperature metamorphism and widespread magma generation. We tentatively link this event with the early heating period on the PTt path presented by *Leloup et al.* [2001] (Figure 14).

[53] The similar metamorphic conditions documented for the ultramafic rocks in the Tan Nguyên area and the surrounding gneisses suggest that the ultramafites were emplaced into the middle crust at the latest at this stage (Figure 15a).

7.2. Initiation of Lateral Extrusion of the Indochina Block

[54] The propagating India-Asia collision triggered lateral extrusion of the Indochina block (Figure 15b), which was accommodated by the RRSZ as a sinistral shear zone [*Tapponnier et al.*, 1982]. Transtensional conditions recorded along the entire DNCV massif are consistent with a progressive clockwise rotation of Indochina and an increasing strike-perpendicular extensional component toward SE [*Leloup et al.*, 2001]. Geochronological data suggest that strike-slip motion started after about 35–32 Ma [*Schärer et al.*, 1994; *Zhang and Schärer*, 1999; *Gilley et al.*, 2003].

7.3. Uplift and Exhumation of the DNCV

[55] Progressive dilation within the RRSZ created a "void," which was infilled by midcrustal gneisses. In this scenario, the SH and SC faults acted as transtensional faults (transiently probably as pure normal faults) that facilitated and accommodated the upward vertical movement of the ductile middle crust. Only the relatively narrow fault zones at the edge of the exhumed DNCV massif recorded the downdip kinematics of this event, while the interior of the massif was uplifted from its originally subhorizontal position [see also *Jolivet et al.*, 2001] and was deformed into an antiformal dome or a core complex type structure (Figure 15c). Unroofing of the DNCV was thus accommodated by a combination of erosion and tectonic removal of the overburden by normal faulting. The upward vertical movement and associated vertical shortening caused the formation of the asymmetric "drag folds" with subhorizontal axial planes (Figure 7). The regional NE–SW extension direction inferred from the orientation and vergence of these folds is

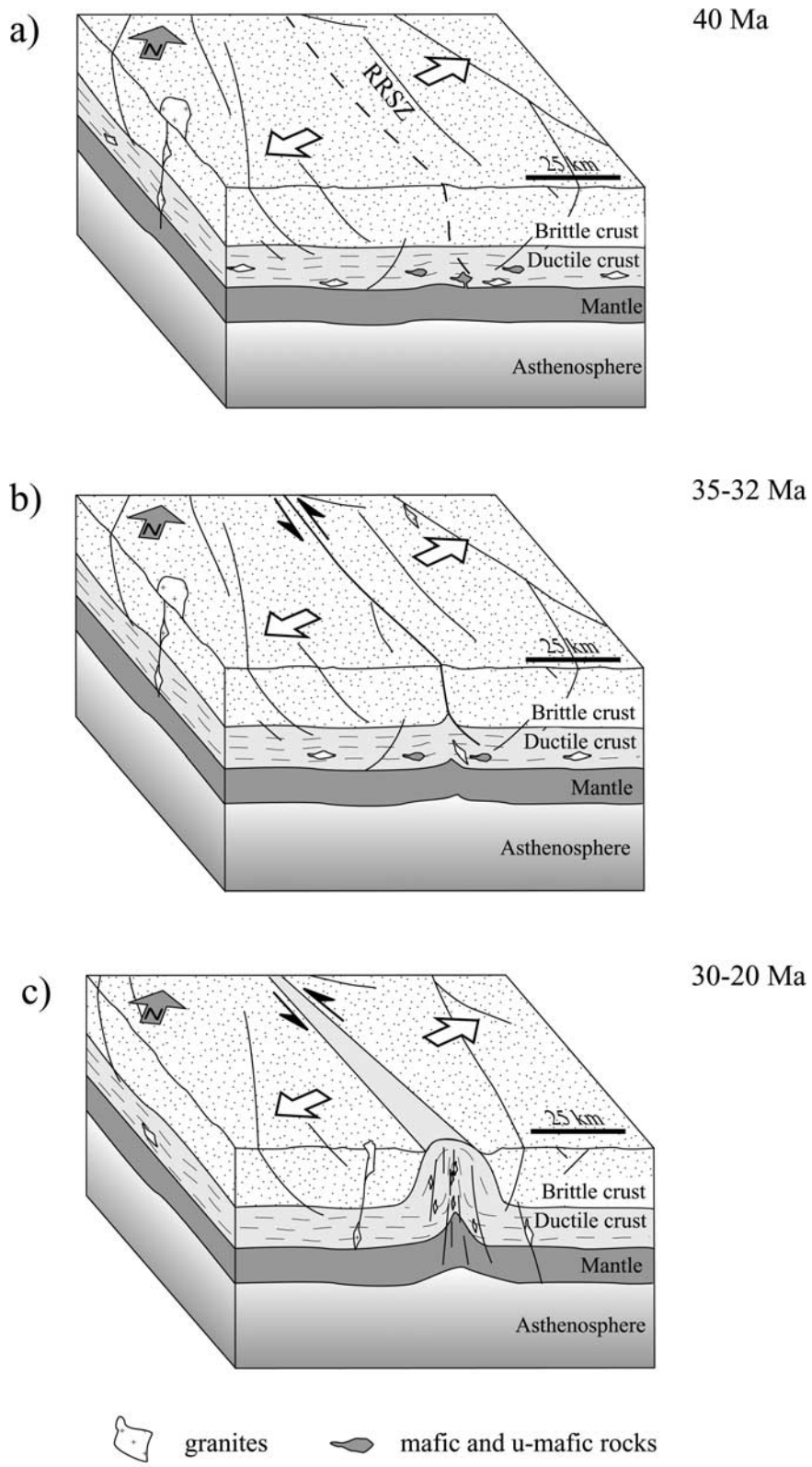

Figure 15. Tectonic scheme for the Red River shear zone (RRSZ) evolution in northern Vietnam. (a–b) Left-lateral shearing combined with strike-perpendicular extension, which caused progressive dilation of the fault zone. (c) Subsequent vertical emplacement of midcrustal gneisses.

consistent with that estimated for the Bu-Khang and the Song Chay domes [*Jolivet et al.*, 2001].

[56] Provided that the currently available time constraints on the initiation of the strike-slip movement are correct, uplift and exhumation of the DNCV occurred very shortly after the onset of the lateral motion and, at least locally, was very rapid. This is inferred from zircon and apatite fission track ages, which yield 30–20 Ma cooling ages in the DNCV massif [*Viola and Anczkiewicz*, 2007]. The fast uplift and exhumation suggested here are in accord with the PTt paths of *Leloup et al.* [2001] and *Nam et al.* [1998], although we postulate higher peak T conditions (Figures 8 and 14). We find a better correlation with the PTt path of *Leloup et al.* [2001] for the early evolution of the DNCV, which explains the pre-left-lateral shearing heating phase postulated by us for the early phase of this model (see above). Additionally, fission track data indicate even faster cooling than that proposed by *Nam et al.* [1998] and *Leloup et al.* [2001]. Such a rapid exhumation could not have been achieved only by means of oblique shearing in a dominantly lateral shear. Instead, it stresses the necessity of a significant component of extension in the history of the southern segment of the Red River shear zone.

8. Conclusions

[57] The Day Nui Con Voi massif bears a record of the RRSZ activity in North Vietnam. It forms a large-scale antiform bounded by the SH and SC faults. These fault zones recorded transtensional left-lateral shear under amphibolite facies conditions, which progressed to greenschist facies conditions. Extensional ductile structures formed under the same metamorphic conditions as the strike-slip-related features. This suggests that they acted contemporaneously although normal movement was spatially partitioned into zones of more intense dip-slip tectonics. Local reworking and obliteration of strike-slip structures by extensional features indicates periods of more intense NE–SW oriented extension along the SH and SC faults, although in an overall transtensional framework.

[58] In our interpretation, the RRSZ evolved from a single, subvertical strike-slip fault, which, due to strike perpendicular extension, was undergoing progressive dilation. The created dilatant space was intruded by the ductile middle crust in the form of a gneissic dome or diapir. Both strike-slip and downdip shearing were accommodated predominantly along the margins of the DNCV massif. The core of the massif thus only exposes uplifted and folded midcrustal gneisses, little affected by the strike-slip and extensional deformation phases.

[59] **Acknowledgments.** This project was funded by Polish Research Grant Committee, project 6PO4D 011 18. We are indebted to Karsten Kunze from the ETH Zurich for help at the texture goniometer. We thank L. Jolivet and two anonymous reviewers for helpful comments. We thank O. Oncken and an anonymous associate editor for efficient handling of the manuscript.

References

Anczkiewicz, R., and M. F. Thirlwall (2003), Improving precision of Sm-Nd garnet dating by H_2SO_4 leaching- a simple solution to phosphate inclusions problem, *J. Geol. Soc. London Spec. Publ.*, *220*, 83–91.

Briais, A., P. Patriat, and P. Tapponnier (1993), Updated interpretation of magnetic anomalies and seafloor spreading stages in the South China Sea: Implications for the Tertiary tectonics of Southeast Asia, *J. Geophys. Res.*, *98*, 6299–6328.

Burchfiel, B. C., Q. Deng, P. Molnar, L. Royden, Y. Wang, P. Zhang, and W. Zhang (1989), Intracrustal detachment within zones of continental deformation, *Geology*, *17*, 748–752.

Chung, S. L., T. Y. Lee, C. H. Lo, P. L. Wang, C. Y. Chen, T. Y. Nguyen, T. H. Tran, and G. Wu (1997), Intraplate extension prior to continental extrusion along the Ailao Shan-Red River shear zone, *Geology*, *25*, 311–314.

Evans, B. W., and B. R. Frost (1975), Chrome-spinel in progressive metamorphism - a preliminary analysis, *Geochim. Cosmochim. Acta*, *39*, 959–972.

Garnier, V., G. Giuliani, H. Maluski, D. Ohnenstetter, T. P. Trong, V. H. Quang, L. P. Van, T. V. Van, and D. Schwarz (2002), Ar-Ar ages in phlogopites from marble-hosted ruby deposits in northern Vietnam: Evidence for Cenozoic ruby formation, *Chem. Geol.*, *188*, 33–49.

General Geological Department of the Democratic Republic of Vietnam (1973), Geological map of Vietnam (the north part), scale 1:1,000,000, Hanoi.

General Geological Directorate (1978), Geological map of the Socialist Republic of Vietnam, scale 1:200,000, Geol. Surv. Inter-Group, Hanoi.

Gilley, L. D., T. M. Harrison, P. H. Leloup, F. J. Ryerson, O. M. Lovera, and J. Wang (2003), Direct dating of left-lateral deformation along the Red River shear zone, China and Vietnam, *J. Geophys. Res.*, *108*(B2), 2127, doi:10.1029/2001JB001726.

Harrison, T. M., P. H. Leloup, F. J. Ryerson, P. Tapponnier, and C. Wenji (1996), Diachronous initiation of transtension along the Ailao Shan-Red River shear zone, Yunnan and Vietnam, in *The Tectonic Evolution of Asia*, edited by A. Yin and T. M. Harrison, pp. 208–225, Cambridge Univ. Press, New York.

Jenkins, D. M., and J. V. Chernosky (1986), Phase equilibria and crystallochemical properties of Mg chlorite, *Am. Mineral.*, *71*, 924–936.

Jolivet, L., H. Maluski, O. Byssac, B. Goffé, T. P. Truong, and N. V. Vuong (1999), The Oligo-Miocene Bu-Khang extensional gneiss dome in North Vietnam, geodynamic implications, *Geology*, *27*, 67–70.

Jolivet, L., O. Beyssac, B. Goffé, D. Avigad, C. Lepvrier, H. Maluski, and T. T. Thang (2001), Oligo-Miocene midcrustal subhorizontal shear zone in Indochina, *Tectonics*, *20*, 46–57.

Katzir, Y., D. Avigad, A. Matthews, Z. Garfunkel, and B. W. Evans (1999), Origin and metamorphism of ultrabasic rocks associated with a subducted continental margin, Naxos (Cyclades, Greece), *J. Metamorph. Geol.*, *17*, 301–318.

Kruhl, J. H. (1996), Prism- and basal-plane parallel subgrain boundaries in quartz: A microstructural geothermobarometer, *J. Metamorph. Geol.*, *14*, 581–589.

Law, R. D. (1990), Crystallographic fabrics: A selective review of their applications to research in structural geology, in *Deformation Mechanisms, Rheology and Tectonics*, edited by R. J. Knipe and E. H. Rutter, *Geol. Soc. Spec. Publ.*, *54*, 335–352.

Le Breton, N., and A. B. Thompson (1988), Fluid absent (dehydration) melting of biotite in metapelites in the early stages of crustal anatexis, *Contrib. Mineral. Petrol.*, *99*, 226–237.

Leloup, P. H., and J. R. Kienast (1993), High-temperature metamorphism in a major strike-slip shear zone: The Ailao Shan-Red River, People's Republic of China, *Earth Planet. Sci. Lett.*, *118*, 213–234.

Leloup, P. H., R. Lacassin, P. Tapponnier, U. Schaerer, Z. Dalai, L. Xiaohan, Z. Liangshang, J. Shaocheng, and P. T. Trinh (1995), The Ailao Shan-Red River shear zone (Yunnan, China), Tertiary transform boundary of Indochina, *Tectonophysics*, *251*, 3–84.

Leloup, P. H., N. Arnaud, R. Lacassin, J. R. Kienast, T. M. Harrison, T. P. Trong, A. Replaumaz, and P. Tapponnier (2001), New constraints on the structure, thermochronology and timing of the Ailao Shan-Red River shear zone, SE Asia, *J. Geophys. Res.*, *106*, 6683–6732.

Mainprice, D., J. L. Bouchez, P. Blumenfeld, and J. M. Tubia (1986), Dominant c-slip in naturally deformed quartz: Implications for dramatic plastic softening at high temperature, *Geology*, *14*, 819–822.

Malavieille, J. (1987), Extensional shearing deformation and kilometer-scale "a"-type folds in a Cordilleran metamorphic core complex (Raft River Mountains, northwestern Utah, *Tectonics*, *6*, 423–448.

Maluski, H., C. Lepvrier, L. Jollivet, A. Carter, D. Roques, O. Beyssac, T. T. Tang, N. D. Thang, and D. Avigad (2001), Ar-Ar and fission-track ages in the Song Chay Massif: Early Triassic and Cenozoic tectonics in northern Vietnam, *J. Asian Earth Sci.*, *19*, 233–248.

Nagy, E. A., U. Schärer, and N. T. Minh (2000), Oligo-Miocene granitic magmatism in central Vietnam

and implications for continental deformation in Indochina, *Terra Nova*, *12*(2), 67–76.

Nam, T. N., M. Toriumi, and T. Itaya (1998), P-T-t paths and post-metamorphic exhumation of the Day Nui Con Voi shear zone in Vietnam, *Tectonophysics*, *290*, 299–318.

Nguyen, H., M. F. J. Flower, and R. W. Carlson (1996), Major, trace element, and isotopic compositions of Vietnamese basalts: Interaction of hydrous EM1-rich asthenosphere with thinned Eurasian lithosphere, *Geochim. Cosmochim. Acta*, *60*, 4329–4351.

Powell, R., and T. J. B. Holland (1988), An internally consistent dataset with uncertainties and correlations: Applications to geobarometry, worked examples and a computer program, *J. Meteorol. Geol.*, *6*, 173–204.

Replumaz, A., R. Lacassin, P. Tapponier, and P. H. Leloup (2001), Large river offsets and Plio-Quaternary dextral slip rate on the Red River fault (Yunnan, China), *J. Geophys. Res.*, *106*, 819–836.

Schärer, U., P. Tapponnier, R. Lacassin, P. H. Leloup, D. Zhong, and S. Ji (1994), Duration of the strike-slip movements in large shear zones: The Red River belt, China, *Earth Planet. Sci. Lett.*, *97*, 379–397.

Schmid, S. M., and M. Casey (1986), Complete fabric analysis of some commonly observed quartz c-axis patterns, in *Mineral and Rock Deformation: Laboratory Studies*, *Geophys. Monogr. Ser.*, vol. 36, edited by B. E. Hobbs and H. C. Heard, pp. 263–286, AGU, Washington, D. C.

Schoenbohm, L. M., K. X. Whipple, B. C. Burchfiel, and L. Chen (2004), Geomorphic constraints on surface uplift, exhumation, and plateau growth in the Red River region, Yunnan province, China, *Geol. Soc. Am. Bull.*, *116*, 895–909.

Simpson, C. (1985), Deformation of granitic rocks across the brittle-ductile transition, *J. Struct. Geol.*, *7*, 503–511.

Stipp, M., H. Stünitz, R. Heilbronner, and S. M. Schmid (2002), The eastern Tonale fault zone: A natural laboratory for crystal plastic deformation of quartz over a temperature range from 250 to 700°C, *J. Struct. Geol.*, *12*, 1861–1884.

Tapponnier, P., G. Peltzer, and A. Y. Ledain (1982), Propagating extrusion tectonics in Asia: New insights from simple experiments with plasticine, *Geology*, *10*, 611–616.

Tapponnier, P., G. Peltzer, and R. Armijo (1986), On the mechanics of the collision between India and Asia, *Geol. Soc. Spec. Publ.*, *19*, 115–157.

Tapponnier, P., R. Lacassin, P. H. Leloup, U. Schaerer, D. Zhong, H. Wu, X. Liu, S. Ji, L. Zhang, and J. Zhong (1990), The Ailao Shan/Red River metamorphic belt; Tertiary left-lateral shear between Indochina and south China, *Nature*, *343*, 431–437.

Thompson, A. B. (1982), Dehydration melting of politic rocks and the generation of H2O-undersautrated granitic liquidus, *Am. J. Sci.*, *282*, 1567–1595.

Trommsdorff, V., and B. W. Evans (1974), Alpine metamorphism of peridotitic rocks, *Schweiz. Mineral. Petrogr. Mitt.*, *54*, 333–352.

Tullis, J. (1977), Preferred orientation of quartz produced by slip during plane strain, *Tectonophysics*, *39*, 87–102.

Ulmer, P., and V. Trommsdorff (1999), Phase relations of hydrous mantle subducting to 300 km, in *Mantle Petrology: Field Observations and High Pressure Experimentation: A Tribute to Francis R. (Joe) Boyd*, edited by Y. Fei, C. M. Bertka, and B. O. Mysen, *Spec. Publ. Geochem. Soc.*, *6*, 259–281.

Vernon, R. H. (1975), Deformation and recrystallization of a plagioclase grain, *Am. Mineral.*, *60*, 884–888.

Vernon, R. H., and R. H. Flood (1988), Contrasting deformation of S- and I-type granitoids in the Lachlan fold belt, eastern Australia, *Tectonophysics*, *147, 127–143.*

Viola, G., and R. Anczkiewicz (2007), Exhumation history of the Red River shear zone in northern Vietnam: Insights from zircon and apatite fission-track analysis, *J. Asian Earth. Sci.*, in press.

Wang, E., and B. C. Burchfiel (1997), Interpretation of Cenozoic tectonics in the right lateral accommodation zone between the Ailao Shan Shear zone and the eastern Himalayan syntaxis, *Int. Geol. Rev*, *39*, 191–212.

Wang, P. L., C. H. Lo, T. Y. Lee, S. L. Chung, C. Y. Lan, and T. Y. Nguyen (1998), Thermochronological evidence for the movement of the Ailao Shan-Red River shear zone: A perspective from Vietnam, *Geology*, *26*, 887–890.

Wang, P. L., C. H. Lo, S. L. Chung, T. Y. Lee, C. Y. Lan, and T. V. Thang (2000), Onset timing of left-lateral movement along the Ailao Shan-Red River Shear Zone: ^{40}Ar-^{39}Ar dating constraint from the Nam Dinh Area, northeastern Vietnam, *J. Asian Earth Sci.*, *18*, 281–292.

Wysocka, A., and A. Świerczewska (2003), Alluvial deposits from the strike-slip fault Lo River Basin (Oligocene/Miocene), Red River Fault Zone, north–western Vietnam, *J. Asian Earth Sci.*, *21*, 1097–1112.

Zhang, L. S., and U. Schärer (1999), Age and origin of magmatism along the Cenozoic Red River shear belt, China, *Contrib. Mineral. Petrol.*, *134*, 67–85.

R. Anczkiewicz and N. Q. Quong, Institute of Geological Sciences, Polish Academy of Sciences, Kraków Research Centre, ul Senacka 1, 31-002 Kraków, Poland. (ndanczki@cyf-kr.edu.pl)

O. Müntener, Institute of Mineralogy and Geochemistry, University of Lausanne, Anthropole, CH-1015 Lausanne, Switzerland.

M. F. Thirlwall, Department of Geology, Royal Holloway, University of London, Egham TW20 0EX, UK.

I. M. Villa, Institut für Geologie, Universität Bern, Baltzerstr. 1, CH-3012 Bern, Switzerland.

G. Viola, Geological Survey of Norway, Trondheim, N-7491, Norway.